LVK-O4a以降のイベントに対するAuto-Regressive法を用いたリングダウン波解析

Ringdown gravitational-wave data analysis with auto-regression method:
Test of general relativity with O4a data and after

真貝寿明(大阪工大)
Hisaaki Shinkai (OIT)
https://www.oit.ac.jp/labs/is/system/shinkai/

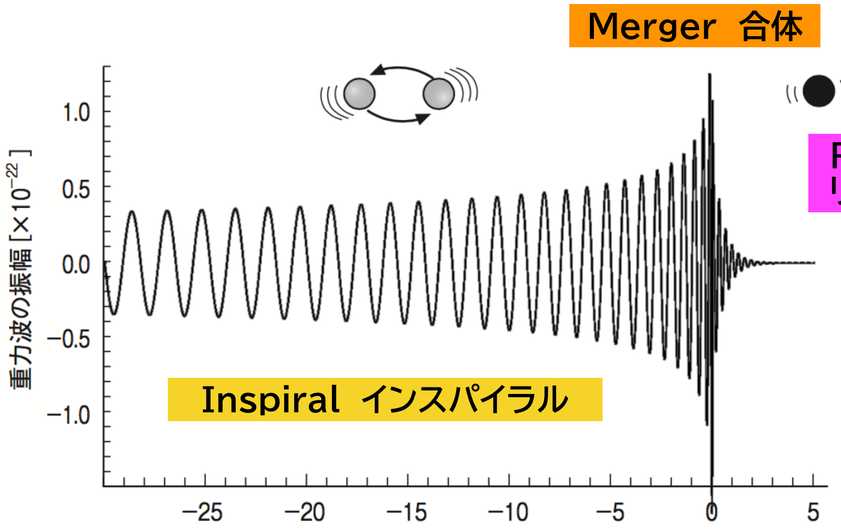

“リングダウン部分”は極めて短時間で減衰
（減衰周期 21.7 ms for 62.7 Msun, a=0.68）

$$t_{M_f} = (1+z)MG/c^3$$

$$t_{M_f}(M = 62.7M_\odot, z = 0.09) = 0.337\mathrm{ms}$$

独立に抽出するには工夫が必要.

➡自己回帰モデル(Auto-Regressive model)

BH 準固有振動 (quasi-normal modes)
⬅ BH 摂動 in GR
➡ (M, a)

強い重力場の影響
➡ GR検証にもっとも優れた状況

GRの予言する周波数・減衰率が見えるのか？
倍音(overtone)の周波数・減衰率が見えるのか？
高次モード(higher modes)の周波数・減衰率が見えるのか？

2022年9月物理学会　AR法は実データで使えるか？ Yes

2023年3月物理学会　O3bまでの実データ・リングダウン波解析

➡➡ リングダウン波の開始時刻はいつか 合体後3ms-5ms

➡➡ 高次モード, 高調波モードはみつかるか GW190412, GW190814 Not yet

➡➡ GRと矛盾しないか consistent

本日　O4a+現在までの実データ・リングダウン波解析

突発性重力波は, GWTC4カタログで観測数が倍増して 176 例

重　力　波

重力波の生成機構　一般相対性理論によれば，大質量でコンパクトな天体が加速度運動することにより，重力波が発生する．重力波源としては連星の合体や超新星爆発，非球対称な星の高速回転や，宇宙初期に起源を持つ重力波が宇宙空間を伝播していると考えられる．これらのうち，データとの相関解析を可能にする波形予測ができるのは，連星合体からの重力波である．十分に合体前はニュートン力学に相対論補正を加えたポスト・ニュートン展開により，合体前後は数値シミュレーションにより，合体後ブラックホールが生じる場合にはブラックホール時空の摂動によっても波形モデルが得られる．これらのモデルと重力波干渉計で得られる信号の相関をとることで，連星ブラックホール（以下 BBH）や連星中性子星（BNS），および中性子星・ブラックホール連星（NSBH）の合体現象による重力波の検出，およびパラメータ推定が 2015 年以来可能になった．

重力波の観測　これまでに，米欧のレーザー干渉計 LIGO, Virgo によって，O4a と呼ばれる観測期間終了までに，BBH 波源の重力波が 169 例，BNS 波源が 2 例，NSBH 波源が 3 例，片方が BH で相方が不明なもの 1 例，片方が NS で相方が不明なもの 1 例の合計 176 例が波源のパラメータを含めて報告されている．日本の KAGRA（かぐら）も O3b の最後に共同観測に入った．KAGRA は能登半島地震でのダメージから復帰して 2025 年 6 月に観測を再開した．O4 観測は，2025 年 11 月まで行われた．その後，世界中の干渉計は精度向上のためアップグレードを行い，O5 観測は 2028 年より行われる．

重力波イベントは，観測された年月日を用いて，GW150914 の形で命名される．O3a 期より，時分秒を加えた名称が正式となった．重力波イベントは速報体制が取られ，多波長電磁波追観測が可能になっているが，これまでに波源が特定されたのは GW170817 のみである．

重力波レーザー干渉計の位置と腕の向き

（例えば N 36°W は北から西方に 36° の向きを指す．）

干渉計	所在地	腕長（km）	緯度	経度	X-腕	Y-腕
LIGO Hanford	米国	4	46°27′19″ N	119°24′28″ W	N 36° W	W 36° S
LIGO Livingston	米国	4	30 33 46 N	90 46 27 W	W 18° S	S 18° E
Virgo	欧州	3	43 37 53 N	10 30 16 E	N 19° E	W 19° N
KAGRA	日本	3	36 24 36 N	137 18 36 E	E 28.3° N	N 28.3° W

観測期間（Observing Run，日付は UTC 表示）

観測期	Advanced LIGO	Advanced Virgo	KAGRA
	年 月 日　年 月 日	年 月 日　年 月 日	年 月 日　年 月 日
O1	2015 9 12 - 2016 1 19	—	—
O2	2016 11 30 - 2017 8 25	2017 8 1 - 2017 8 25	—
O3a	2019 4 1 - 2019 9 30	同左	—
O3b	2019 11 1 - 2020 3 27	同左	(O3GK) 2020 4 7 - 2020 4 21
O4a	2023 5 24 - 2024 1 16	—	2023 5 26 - 2023 6 25
O4b	2024 4 10 - 2025 1 28	同左	—
O4c	2025 1 29 - 2025 11 18	同左	2025 6 6 - 2025 11 18

重力波の項
2022年より登場

by 田中貴浩さん＋HS

Gravitational Wave Transient Catalog　（GWTC）

		released	arXiv	ref.	BHBH	NSNS	NSBH	相方不明	total
GWTC-1	O1+O2	2018/12/3	1811.12907	PRX 9 (2019) 031040	10	1			11
GWTC-2	O3a	2020/10/28	2010.14527	PRX 11 (2011) 021053	36	1		2	39
GWTC-2.1	+	2021/8/2	2108.01045		+8-3				5
GWTC-3	O3b	2021/11/5	2111.03606	PRX 13 (2023) 041039	32		3		35
GWTC-4	O4a	2025/8/25	2508.18082		86				86
				total	169	2	3	2	176

突発性重力波は, GWTC4カタログで観測数が倍増して 176 例

O3a

O3b

O4a

	イベント（BBH）	$M_c\ (M_\odot)$	質量比	$\chi_{\rm eff}$	$M_{\rm final}\ (M_\odot)$	距離（Mpc）	$(\Delta\Omega)^2$	SNR	
✔	GW150914	$28.6^{+1.7}_{-1.5}$	0.86	$-0.01^{+0.12}_{-0.13}$	$63.1^{+3.4}_{-3.0}$	440^{+150}_{-170}	250	26	
	GW170814	$24.1^{+1.4}_{-1.1}$	0.82	$0.07^{+0.12}_{-0.12}$	$53.2^{+3.2}_{-2.4}$	600^{+150}_{-220}	92	17.7	
✔	GW190412	$13.3^{+0.5}_{-0.5}$	0.32	$0.21^{+0.12}_{-0.13}$	$35.6^{+4.8}_{-4.5}$	720^{+240}_{-220}	240	19.8	
	GW190521	$63.3^{+19.6}_{-14.6}$	0.58	$-0.14^{+0.5}_{-0.45}$	$147.4^{+40.0}_{-16.0}$	3310^{+2790}_{-1800}	1000	14.3	⊘ too heavy, low freq.
✔	GW190521_074359	$32.8^{+3.2}_{-2.8}$	0.77	$0.1^{+0.13}_{-0.13}$	$72.6^{+6.5}_{-5.4}$	1080^{+580}_{-530}	470	25.9	
	GW191216_213338	$8.33^{+0.22}_{-0.19}$	0.64	$0.11^{+0.13}_{-0.06}$	$18.87^{+2.81}_{-0.93}$	340^{+120}_{-130}	490	18.6	⊘ too light, high freq.
✔	GW200112_155838	$27.4^{+2.6}_{-2.1}$	0.79	$0.06^{+0.15}_{-0.15}$	$60.8^{+5.3}_{-4.3}$	1250^{+430}_{-460}	4300	19.8	
✔	GW200129_065458	$27.2^{+2.1}_{-2.3}$	0.84	$0.11^{+0.11}_{-0.16}$	$60.2^{+4.1}_{-3.2}$	890^{+260}_{-370}	130	26.8	
✔	GW200224_222234	$31.1^{+3.3}_{-2.7}$	0.82	$0.1^{+0.15}_{-0.16}$	$68.7^{+6.7}_{-4.8}$	1710^{+500}_{-650}	50.0	20	
✔	GW200311_115853	$26.6^{+2.4}_{-2.0}$	0.81	$-0.02^{+0.16}_{-0.2}$	$59^{+4.8}_{-3.9}$	1170^{+280}_{-400}	35	17.8	
	GW230627_015337	$6.02^{+0.16}_{-0.07}$	0.70	$0.02^{+0.08}_{-0.03}$	$13.5^{+0.8}_{-0.5}$	310^{+60}_{-130}	99	28.7	⊘ too light, high freq.
✔	GW230814_230901	$26.8^{+0.8}_{-0.9}$	0.85	$-0.01^{+0.05}_{-0.08}$	$58.9^{+1.8}_{-1.8}$	200^{+100}_{-100}	25000	45.9	Livingston only
✔	GW230914_111401	$39.8^{+7.5}_{-6.3}$	0.60	$0.1^{+0.2}_{-0.2}$	$91.5^{+13.9}_{-9.7}$	2600^{+1600}_{-1200}	1600	17.7	
✔	GW230927_153832	$16.4^{+1.4}_{-0.8}$	0.75	$0.02^{+0.07}_{-0.08}$	$36.6^{+3.1}_{-2.1}$	1200^{+400}_{-500}	270	21.5	
	GW231028_153006	$62.0^{+13.0}_{-10.0}$	0.54	$0.4^{+0.2}_{-0.2}$	145^{+27}_{-14}	4100^{+1400}_{-1800}	1200	22.9	⊘ too heavy, low freq.
	GW231123_135430	102^{+12}_{-31}	0.75	$0.3^{+0.2}_{-0.4}$	225^{+26}_{-43}	2200^{+1900}_{-1500}	1200	22.6	⊘ waveform system. err?
✔	GW231206_233901	$28.1^{+2.6}_{-1.7}$	0.76	$-0.05^{+0.13}_{-0.14}$	$63.0^{+4.7}_{-3.3}$	1500^{+300}_{-500}	310	22.9	
✔	GW231226_101520	$32.5^{+1.5}_{-1.3}$	0.88	$-0.09^{+0.08}_{-0.09}$	$71.5^{+3.1}_{-2.5}$	1200^{+200}_{-300}	150	40.7	
	イベント（BNS）	$M_c\ (M_\odot)$	質量比	$\chi_{\rm eff}$	$M_{\rm 全}\ (M_\odot)$	距離（Mpc）	$(\Delta\Omega)^2$	SNR	
	GW170817	$1.186^{+0.001}_{-0.001}$	0.87	$0^{+0.02}_{-0.01}$	—	$40^{+7.0}_{-15.0}$	16	33	too light, high freq.
	GW190425	$1.44^{+0.02}_{-0.02}$	0.62	$0.07^{+0.07}_{-0.05}$	$3.4^{+0.3}_{-0.1}$	150^{+80}_{-60}	8700	12.4	too light, high freq.
	イベント（NSBH）	$M_c\ (M_\odot)$	質量比	$\chi_{\rm eff}$	$M_{\rm 全}\ (M_\odot)$	距離（Mpc）	$(\Delta\Omega)^2$	SNR	
	GW190917_114630	$3.7^{+0.2}_{-0.2}$	0.22	$-0.08^{+0.21}_{-0.43}$	$11.8^{+3.0}_{-2.8}$	720^{+300}_{-310}	2100	8.3	too light, high freq.
	GW200115_042309	$2.43^{+0.05}_{-0.07}$	0.24	$-0.15^{+0.23}_{-0.42}$	$7.4^{+1.7}_{-1.7}$	290^{+150}_{-100}	370	11.3	too light, high freq.
	GW230518_125908	$2.80^{+0.06}_{-0.06}$	0.17	$-0.01^{+0.09}_{-0.11}$	$9.4^{+0.7}_{-0.8}$	240^{+110}_{-100}	520	14.3	too light, high freq.
	イベント（低質量ギャップ天体を含む）	$M_c\ (M_\odot)$	質量比	$\chi_{\rm eff}$	$M_{\rm 全}\ (M_\odot)$	距離（Mpc）	$(\Delta\Omega)^2$	SNR	
	GW190814	$6.11^{+0.06}_{-0.05}$	0.11	$0^{+0.07}_{-0.07}$	$25.7^{+1.3}_{-1.3}$	230^{+40}_{-50}	22	25.3	too light, high freq.
	GW230529_181500	$1.94^{+0.04}_{-0.04}$	0.36	$-0.05^{+0.14}_{-0.15}$	$5.04^{+0.82}_{-0.62}$	200^{+110}_{-100}	24000	11.8	too light, high freq.

O4b (event paper)
PRL135(2025)111403,
PRL136(2025)041403

✔ **GW250114_082203**

$(M, a, z) = (62.7^{+1}_{-1.1}, 0.68^{+0.01}_{-0.01}, 0.09^{+0.01}_{-0.01})$

network SNR = 80 !
ringdown wave (2,2,0)+(2,2,1)
±30% Kerr

Tests of General Relativity with GWTC-4（LVK paper）

the 91 confident signals including 42 events in O4a (FAR<10^{-3}/yr)

parameter range of GWTC3 / GWTC4
(POL: GWTC3 minus GWTC4)

Test	Paper	Section	Quantity	Parameter	Main Result	Improvement
RT	I	4.1	p-value for the presence of a residual signal	p-value	Consistent with uniform dist.	···
IMRCT	I	4.2	Fractional deviation in remnant mass and spin	$\left\{\frac{\Delta M_{\rm f}}{\bar{M}_{\rm f}}, \frac{\Delta\chi_{\rm f}}{\bar{\chi}_{\rm f}}\right\}$	$\left\{0.00^{+0.07}_{-0.06}, -0.05^{+0.11}_{-0.11}\right\}$	$\{2.0, 2.5\}$
SMA	I	4.3	Frac. deviation in amplitude of higher multipole moments	δA_{33}	$-0.21^{+1.82}_{-3.39}$	New
POL	I	5	Bayes factors between different polarization hypotheses	$\log_{10}\mathcal{B}^{X}_{\rm T}$	$-14.72^{+0.59}_{-0.59} - 0.10^{+0.57}_{-0.57}$	0.21 – 10.48
PAR	II	2.1	FTI: PN deformation params	$\lvert\delta\hat{\varphi}_k\rvert$	$\leq 1.6\times10^{-3} - 1.5$	1.2 – 5.5
		2.1	TIGER: PN deformation params	$\lvert\delta\hat{\varphi}_k\rvert$	$\leq 5.3\times10^{-4} - 1.2$	1.3 – 3.9
		2.1	TIGER: Post-inspiral deformation params	$\left\lvert\delta\hat{b}_k\right\rvert, \lvert\delta\hat{c}_k\rvert$	$\leq 7.7\times10^{-3} - 0.28$	Maj. Update
		2.2	PCA: Best-constrained combination of PN deformation params	$\delta\hat{\varphi}^{(1)}_{\rm PCA,FTI}, \delta\hat{\varphi}^{(1)}_{\rm PCA,TIGER}$	$-0.01^{+0.04}_{-0.03}, 0.01^{+0.06}_{-0.06}$	New
SIM	II	2.3	Phenom: Deformation in spin-induced multipole parameter	$\delta\kappa_s$	-19^{+28}_{-34}	1.4
		2.3	EOB: Deformation in spin-induced multipole param	$\delta\kappa_s$	-49^{+95}_{-176}	New
LOSA	II	2.4	Line-of-sight acceleration	$a/c\,[\mathrm{s}^{-1}]$	$0.42^{+2.00}_{-1.87}\times10^{-6}$	New
MDR	II	3.1	Magnitude of dispersion	$\lvert A_\alpha\rvert\,[\mathrm{peV}^{2-\alpha}]$	$\leq (0.01 - 351)\times10^{-22}$	1.48 – 2.88
		3.1	Graviton mass bound	$m_g\,[\mathrm{eV}/c^2]$	$\leq 1.92\times10^{-23}$	1.16
SSB	II	3.2	Constraints on anisotropic birefringent propagation	$\left\lvert k^{(5)}_{00}\right\rvert\,[\mathrm{m}]$	$\leq 1.52\times10^{-14}$	New
RD	III	2.1	PYRING (KerrPostmerger): Frac. dev. in freq. & damp. time	$\left\{\delta\hat{f}_{220}, \delta\hat{\tau}_{220}\right\}$	$\left\{0.10^{+0.23}_{-0.18}, 0.18^{+0.27}_{-0.26}\right\}$	New
		2.2	pSEOBNR: Frac. deviations in frequency & damping time	$\left\{\delta\hat{f}_{220}, \delta\hat{\tau}_{220}\right\}$	$\left\{0.00^{+0.06}_{-0.06}, 0.16^{+0.18}_{-0.16}\right\}$	$\{1.09, 1.52\}$
		2.3	QNMRF: Detection statistic for subdominant ringdown modes	$\mathcal{D} - \mathcal{D}_{1\%}$	221: ≤ 3.1	New
E-WFM	III	3.1	ADA: Bayes factor for IMR plus echoes to IMR only	$\log_{10}\mathcal{B}^{\rm IMRE}_{\rm IMR}$	≤ 1.1	···
		3.1	BHP: Bayes factor for IMR plus echoes to IMR only	$\log_{10}\mathcal{B}^{\rm IMRE}_{\rm IMR}$	≤ 0.2	New
E-MM	III	3.2	BAYESWAVE: Signal-to-noise Bayes factor for echoes	$\log_{10}\mathcal{B}^{\rm signal}_{\rm noise}$	≤ -1.8	···
		3.3	CWB: p-value for the presence of echoes	p-value	Consistent with uniform dist.	New

◀ GW190814 (mass gap+BH)
(Mc=6.1Msun, Mf=25.7Msun)

◀ GW170817 (BNS)

◀ GW231028_153006
(Mc=62Msun, Mf=145Msun)

Tests of General Relativity with GWTC-4（LVK paper）

the 91 confident signals including 42 events in O4a (FAR<10^{-3}/yr)

parameter range of GWTC3 / GWTC4
(POL: GWTC3 minus GWTC4)

Test	Paper	Section	Quantity	Parameter	Main Result	Improvement
RT	I	4.1	p-value for the presence of a residual signal	p-value	Consistent with uniform dist.	···
IMRCT	I	4.2	Fractional deviation in remnant mass and spin	$\left\{\frac{\Delta M_f}{\bar{M}_f}, \frac{\Delta\chi_f}{\bar{\chi}_f}\right\}$	$\{0.00^{+0.07}_{-0.06}, -0.05^{+0.11}_{-0.11}\}$	$\{2.0, 2.5\}$
SMA	I	4.3	Frac. deviation in amplitude of higher multipole moments	δA_{33}	$-0.21^{+1.82}_{-3.39}$	New
POL	I	5	Bayes factors between different polarization hypotheses	$\log_{10}\mathcal{B}^X_T$	$-14.72^{+0.59}_{-0.59} - 0.10^{+0.57}_{-0.57}$	$0.21 - 10.48$

◀ GW190814 (mass gap+BH)
(Mc=6.1Msun, Mf=25.7Msun)

Residual test

consistency of the residuals with noise

Inspiral-Merger–Ringdown consistency

$$\frac{\Delta M_f}{\bar{M}_f} = 2\frac{M_f^I - M_f^{PI}}{M_f^I + M_f^{PI}}, \quad \frac{\Delta\chi_f}{\bar{\chi}_f} = 2\frac{\chi_f^I - \chi_f^{PI}}{\chi_f^I + \chi_f^{PI}},$$

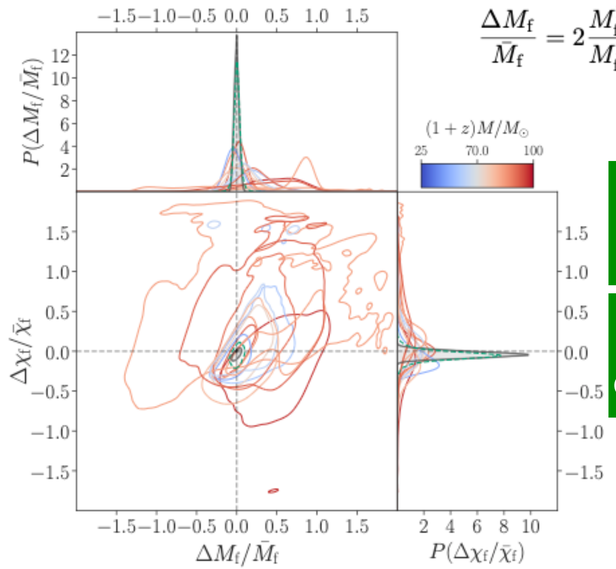

consistent
inspiral vs post-inspiral

no evidence for
deviations from models

Subdominant Multipole Amplitudes

$$h(t,\theta_{JN},\boldsymbol{\lambda}) = \sum_{m=\pm2} Y^{2m}_{-2}(\theta_{JN},0)\,h_{2m}(t,\boldsymbol{\lambda}) + \sum_{m=\pm1}(1+\delta A_{21})Y^{2m}_{-2}(\theta_{JN},0)\,h_{2m}(t,\boldsymbol{\lambda}) + \sum_{m=\pm3}(1+\delta A_{33})Y^{3m}_{-2}(\theta_{JN},0)\,h_{3m}(t,\boldsymbol{\lambda}) + \sum_{\text{other HOM}} Y^{\ell m}_{-2}(\theta_{JN},0)\,h_{\ell m}(t,\boldsymbol{\lambda}). \quad (10)$$

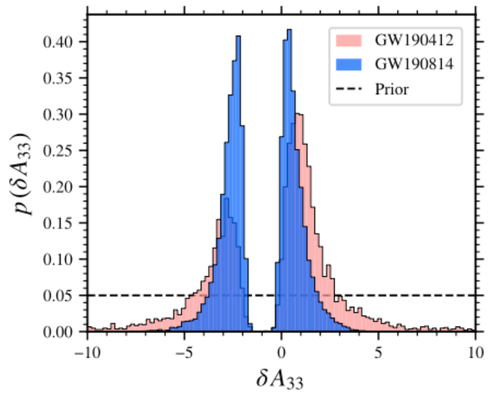

Polarization Test

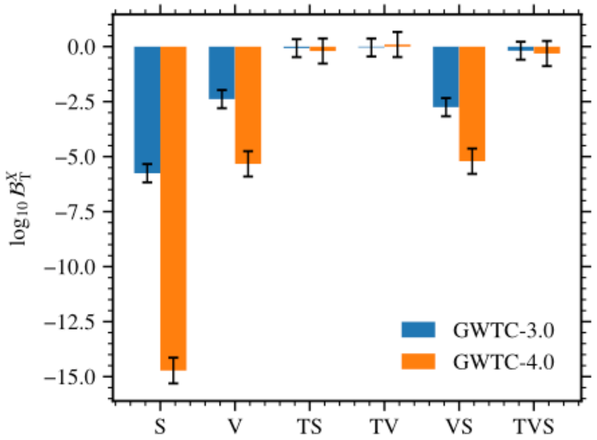

no evidence for
deviations from the GR

Tests of General Relativity with GWTC-4（LVK paper）

RD	III	2.1	PYRING (KerrPostmerger): Frac. dev. in freq. & damp. time	$\{\delta\hat{f}_{220}, \delta\hat{\tau}_{220}\}$	$\{0.10^{+0.23}_{-0.18}, 0.18^{+0.27}_{-0.26}\}$	New
		2.2	pSEOBNR: Frac. deviations in frequency & damping time	$\{\delta\hat{f}_{220}, \delta\hat{\tau}_{220}\}$	$\{0.00^{+0.06}_{-0.06}, 0.16^{+0.18}_{-0.16}\}$	$\{1.09, 1.52\}$
		2.3	QNMRF: Detection statistic for subdominant ringdown modes	$\mathcal{D} - \mathcal{D}_{1\%}$	221: ≤ 3.1	New
E-WFM	III	3.1	ADA: Bayes factor for IMR plus echoes to IMR only	$\log_{10} \mathcal{B}^{\mathrm{IMRE}}_{\mathrm{IMR}}$	≤ 1.1	...
		3.1	BHP: Bayes factor for IMR plus echoes to IMR only	$\log_{10} \mathcal{B}^{\mathrm{IMRE}}_{\mathrm{IMR}}$	≤ 0.2	New
E-MM	III	3.2	BAYESWAVE: Signal-to-noise Bayes factor for echoes	$\log_{10} \mathcal{B}^{\mathrm{signal}}_{\mathrm{noise}}$	≤ -1.8	...
		3.3	CWB: p-value for the presence of echoes	p-value	Consistent with uniform dist.	New

◀ GW231028_153006
(Mc=62Msun, Mf=145Msun)

(PYRING) a time-domain analysis that examines only the post-merger signal

no statistically significant evidence for the presence of multiple modes
for all events, there were 90% CL overlaps with the results of the IMR analysis

finds a shifts towards larger frequencies and damping times. However, ...

(pSEOBNR) a frequency-domain analysis that considers the entire signal

finds a shift toward higher GR quantiles for the damping time when O4a events are added to the analysis. However, ...

Table 4. GR quantiles for combined pSEOBNR results

Catalog	Joint $Q^{\mathrm{2D}}_{\mathrm{GR}}$	Hierarchical $Q^{\mathrm{1D},\mu_{\delta\hat{\tau}_{220}}}_{\mathrm{GR}}$	Hierarchical $Q^{\mathrm{4D}}_{\mathrm{GR}}$
GWTC-3.0	$93.8^{+6.1}_{-20.0}\%$	$94.9^{+4.4}_{-18.2}\%$	$66.1^{+31.9}_{-34.6}\%$
GWTC-4.0	$98.6^{+1.4}_{-9.4}\%$	$99.3^{+0.7}_{-4.5}\%$	$85.1^{+14.9}_{-19.7}\%$

(QNMRF) a time-domain analysis that filters out specific QNMs from the post-merger signal

finds that for GW231028_153006 the detection statistic favors the presence of the 221 mode. However, possible systematic effects cannot be ruled out, and overtone analyses are particularly sensitive to such systematic uncertainties.

➡ ところどころ歯切れの悪い説明もあるが, GRとconsistentという結論

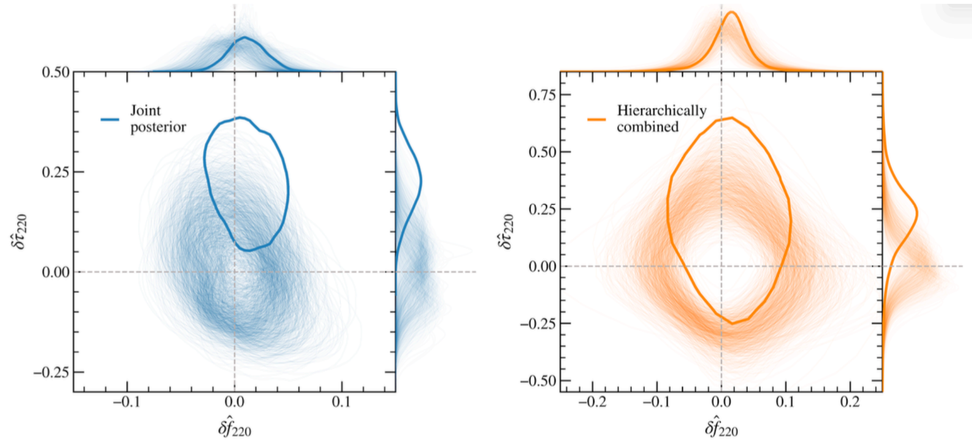

GW250114_0822203

network SNR = 80 !

PHYSICAL REVIEW LETTERS **135,** 111403 (2025)

Editors' Suggestion | Featured in Physics

GW250114: Testing Hawking's Area Law and the Kerr Nature of Black Holes

A. G. Abac *et al.*[*]
(LIGO Scientific, Virgo, and KAGRA Collaborations)

(Received 13 August 2025; revised 25 August 2025; accepted 26 August 2025; published 10 September 2025)

The gravitational-wave signal GW250114 was observed by the two LIGO detectors with a network matched-filter signal-to-noise ratio of 80. The signal was emitted by the coalescence of two black holes with near-equal masses $m_1 = 33.6^{+1.2}_{-0.8} M_\odot$ and $m_2 = 32.2^{+0.8}_{-1.3} M_\odot$, and small spins $\chi_{1,2} \leq 0.26$ (90% credibility) and negligible eccentricity $e \leq 0.03$. Postmerger data excluding the peak region are consistent with the dominant quadrupolar ($\ell = |m| = 2$) mode of a Kerr black hole and its first overtone. We constrain the modes' frequencies to ±30% of the Kerr spectrum, providing a test of the remnant's Kerr nature. We also examine Hawking's area law, also known as the second law of black hole mechanics, which states that the total area of the black hole event horizons cannot decrease with time. A range of analyses that exclude up to five of the strongest merger cycles confirm that the remnant area is larger than the sum of the initial areas to high credibility.

PHYSICAL REVIEW LETTERS **136,** 041403 (2026)

Editors' Suggestion | Featured in Physics

Black Hole Spectroscopy and Tests of General Relativity with GW250114

A. G. Abac *et al.*[*]
(The LIGO Scientific Collaboration, The Virgo Collaboration, and The KAGRA Collaboration)

(Received 12 September 2025; revised 24 October 2025; accepted 18 November 2025; published 29 January 2026)

The binary black hole signal GW250114, the loudest gravitational wave detected to date, offers a unique opportunity to test Einstein's general relativity (GR) in the high-velocity, strong-gravity regime and probe whether the remnant conforms to the Kerr metric. Upon perturbation, black holes emit a spectrum of damped sinusoids with specific, complex frequencies. Our analysis of the postmerger signal shows that at least two quasinormal modes are required to explain the data, with the most damped remaining statistically significant for about one cycle. We probe the remnant's Kerr nature by constraining the spectroscopic pattern of the dominant quadrupolar ($\ell = m = 2$) mode and its first overtone to match the Kerr prediction to tens of percent at multiple postpeak times. The measured mode amplitudes and phases agree with a numerical-relativity simulation having parameters close to GW250114. By fitting a parametrized waveform that incorporates the full inspiral-merger-ringdown sequence, we constrain the fundamental ($\ell = m = 4$) mode to tens of percent and bound the quadrupolar frequency to within a few percent of the GR prediction. We perform a suite of tests—spanning inspiral, merger, and ringdown—finding constraints that are comparable to, and in some cases 2–3 times more stringent than those obtained by combining dozens of events in the fourth Gravitational-Wave Transient Catalog. These results constitute the most stringent single-event verification of GR and the Kerr nature of black holes to date, and outline the power of black-hole spectroscopy for future gravitational-wave observations.

$$(M, a, z) = (62.7^{+1}_{-1.1}, 0.68^{+0.01}_{-0.01}, 0.09^{+0.01}_{-0.01})$$

$$33.6^{+1.2}_{-0.8} M_\odot + 32.2^{+0.8}_{-1.3} M_\odot$$

$$\chi_1 \leq 0.24, \chi_2 \leq 0.26, e \leq 0.03$$

$$h_+ - i h_\times = \sum_{\substack{\ell \geq 2 \\ 0 \leq m \leq \ell \\ n \geq 0}} e^{-t/\tau_{\ell mn}} \left(A^{\mathrm{R}}_{\ell mn} e^{-2\pi i f_{\ell mn} t} + A^{\mathrm{L}}_{\ell mn} e^{2\pi i f_{\ell mn} t} \right)$$

ringdown wave (2,2,0)+(2,2,1)　±30% Kerr
(2,2,2)まで見えたとは断言し難い

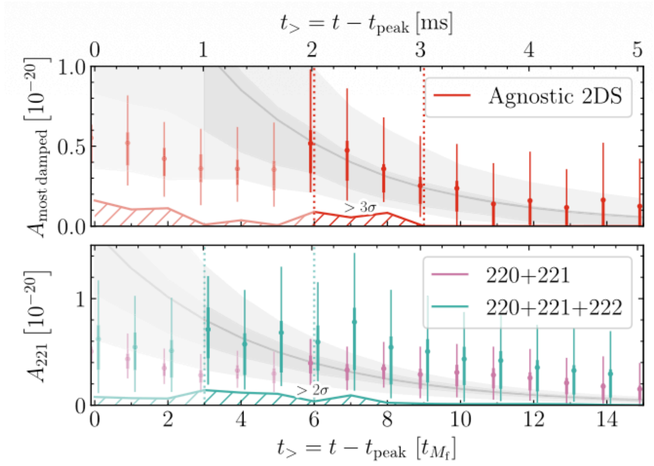

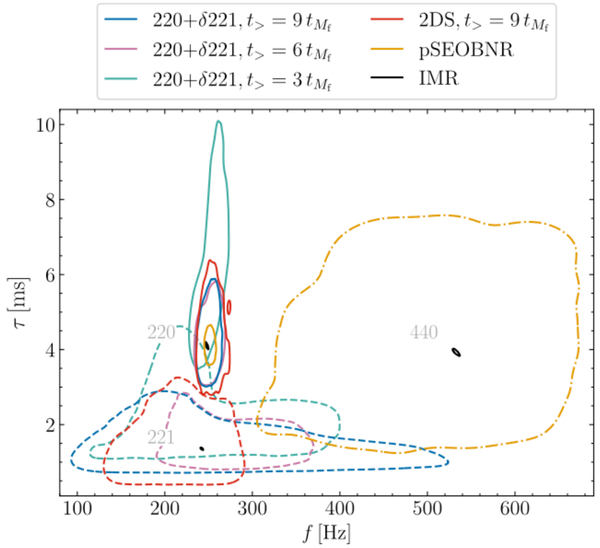

$$f_{\ell m0} = f^{\mathrm{GR}}_{\ell m0}(1 + \delta \hat{f}_{\ell m0}), \quad \tau_{\ell m0} = \tau^{\mathrm{GR}}_{\ell m0}(1 + \delta \hat{\tau}_{\ell m0})$$

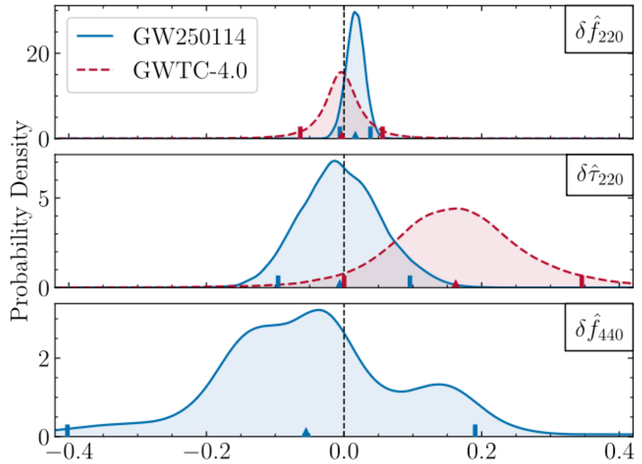

IMR解析にて，(4,4,0)を入れてもGRとconsistent

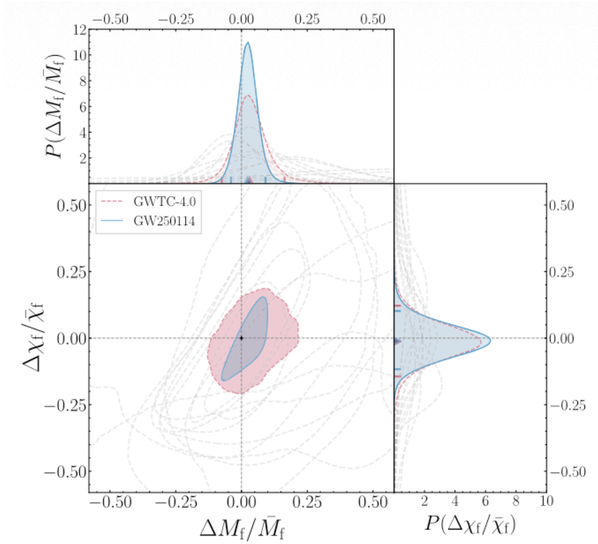

自己回帰モデル　Auto-Regressive model (Method, general)

Fitting data with linear func.

$$x_n = a_1 x_{n-1} + a_2 x_{n-2} + \cdots + a_M x_{n-M} + \varepsilon = \sum_{j=1}^{M} a_j x_{n-j} + \varepsilon$$

e.g. $x_n = A e^{-rn\Delta t}\cos(\omega n \Delta t)$

$$Z_1 = e^{-(r-j\omega)\Delta t}, \quad Z_2 = e^{-(r+j\omega)\Delta t} \Rightarrow x_n = \frac{A}{2}(Z_1^n + Z_2^n) = (Z_1+Z_2)x_{n-1} - Z_1 Z_2 x_{n-2}$$

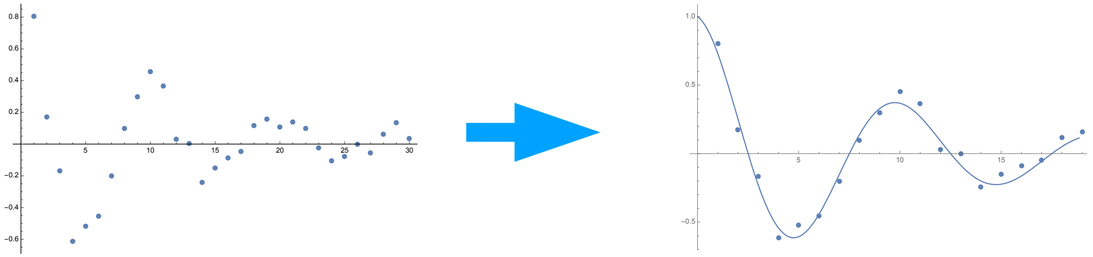

can be applied also to noisy data by adjusting *M*

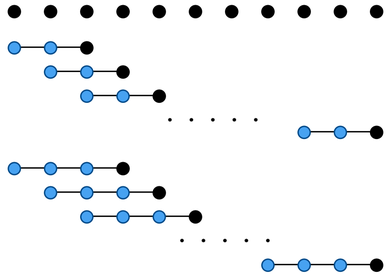

- find a_j (Burg method)
- find M (FPE final prediction error method)
- re-construct wave signal from fitted function
- apply FFT with arbitrary precision.

power spectrum

$$p(f) = \frac{\sigma^2}{\left|1 - \sum_{j=1}^{M} a_j e^{-I2\pi j f \Delta t}\right|^2}$$

characteristic eq.

$$f(z) = 1 - \sum_{j=1}^{M} a_j z^j = 0$$

$|z_k|$ says amplitude,
$\arg(z_k)$ says frequency.

P(f)

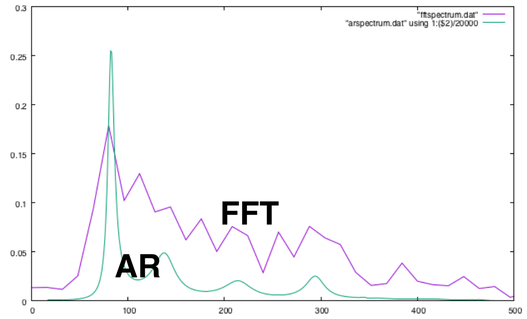

freq.　[mock data, SNR=40, inspiral part]

The order M can be fixed at 2〜8.

**Even for short segment,
AR model shows precise power-spectrum.**

自己回帰モデル(重力波解析手順) Auto-Regressive model (GW)

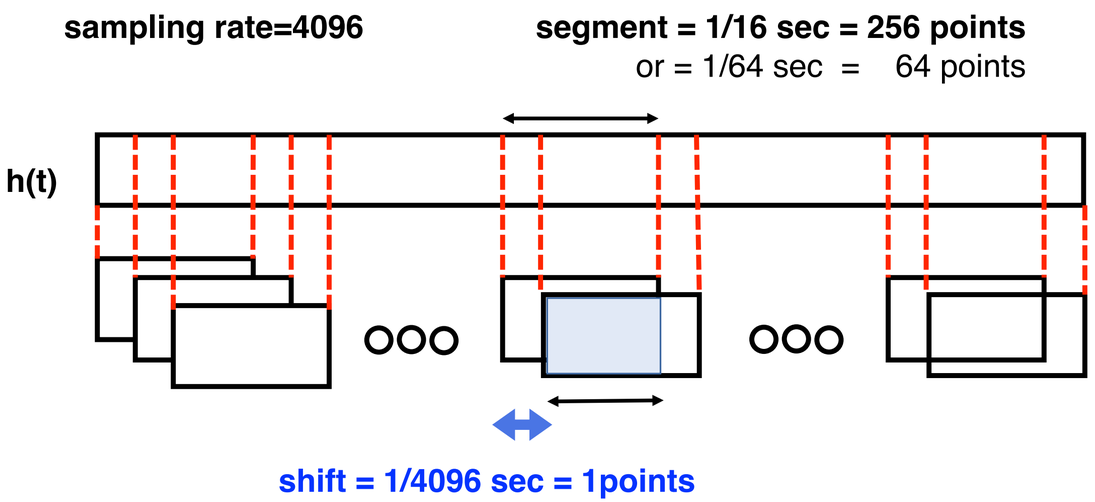

干渉計のイベントが報告されたデータ(ホワイトニング後)で，合体時刻後のデータを解析する．
自己回帰モデルを用いて，周波数 $f_{\rm real}$ と振幅減衰率 τ (= $f_{\rm imag}$)を特定する．

モデルを仮定せずに，実データのみに基づく　検出器ごと独立に解析

一定周波数となっているものを探す．（リングダウンモード !?）
$f_{\rm real}$ の散らばりが1σ以内，τ(= $f_{\rm imag}$)の散らばりが1.25σ以内のものを抽出

各モードの存在時間が抽出可能

各データセグメントで，複数の (f, τ) を抽出可能

複数のモードを抽出可能

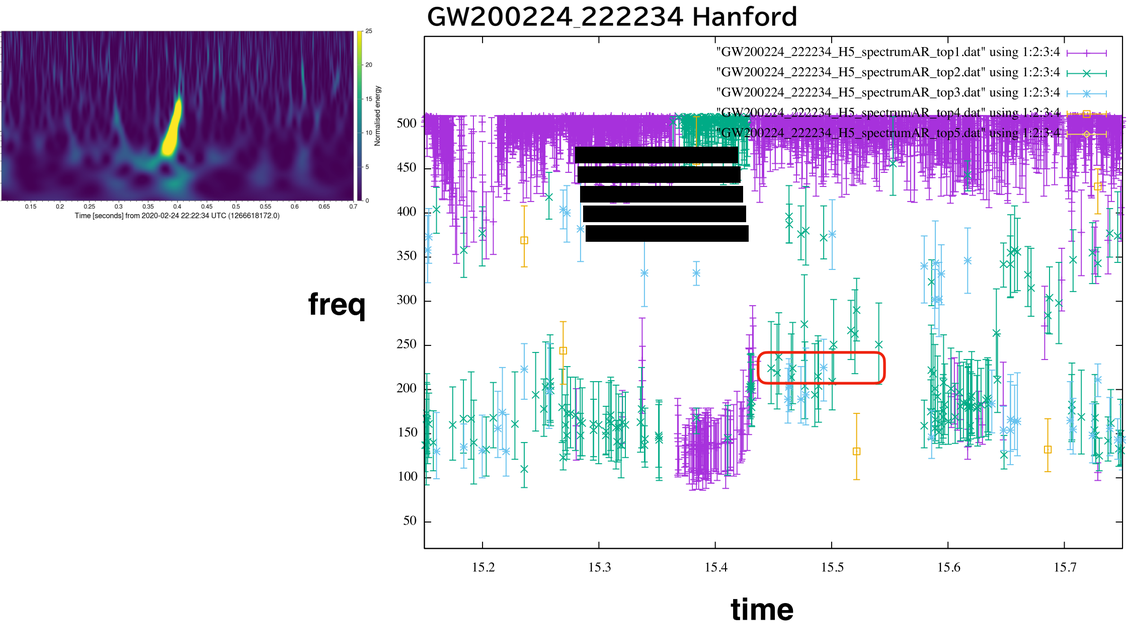

LVK catalog の 最終的なBHの (M_f, a_f) + 赤方偏移 z のデータから
検出データのリングダウンモード (f, τ) を求め，GR値とみなす

$$f_R = f_1 + f_2(1-a)^{f_3}$$
$$Q \equiv \frac{f_R}{2f_I} = q_1 + q_2(1-a)^{q_3}$$

$$f_{\rm qnm}[{\rm Hz}] = \frac{c^3}{2\pi GM} f_R \sim 32314.1 \left(\frac{M_\odot}{M}\right) f_R.$$

$$a = 1 - \left(\frac{Q-q_1}{q_2}\right)^{1/q_3}$$
$$M[M_\odot] = 32314.1 \times \frac{f_1 + f_2(1-a)^{f_3}}{f_{\rm qnm}[{\rm Hz}]}$$

Berti, Cardoso & Will PRD 73, 064030 (2006).

AR法はリングダウン波を抽出しているか
3干渉計(Hanford, Livingston, Virgo) で合致した値になるか
LVK catalogと合致した値になるか

リングダウン波の開始時刻はいつか
高次モード，高調波モードはみつかるか
GRと矛盾しないか

重力波到来方向の特定から，各検出器での連星「合体」重力波通過時刻を補正

GW150914の例

Hanford

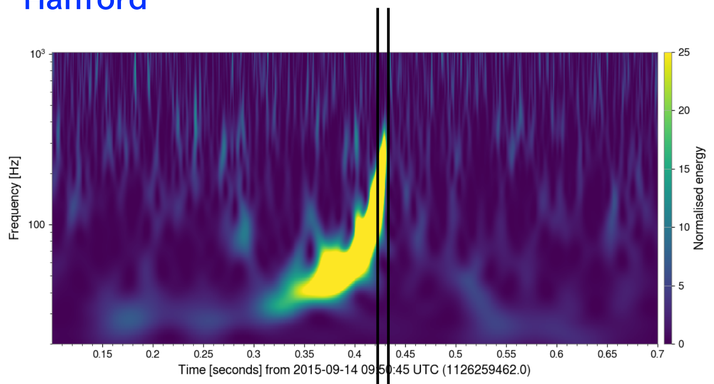

Livingston

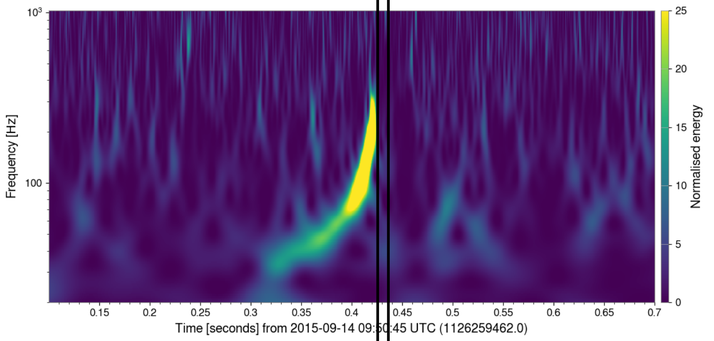

with a 35–350 Hz bandpass filter to suppress large fluctuations outside the detectors' most sensitive frequency band, and band-reject filters to remove the strong instrumental spectral lines seen in the Fig. 3 spectra. *Top row, left:* H1 strain. *Top row, right:* L1 strain. GW150914 arrived first at L1 and $6.9^{+0.5}_{-0.4}$ ms later at H1; for a visual comparison, the H1 data are also shown, shifted in time by this amount and inverted (to account for the detectors' relative orientations). *Second row:* Gravitational-wave strain projected onto each

PRL 116 (2016) 061102

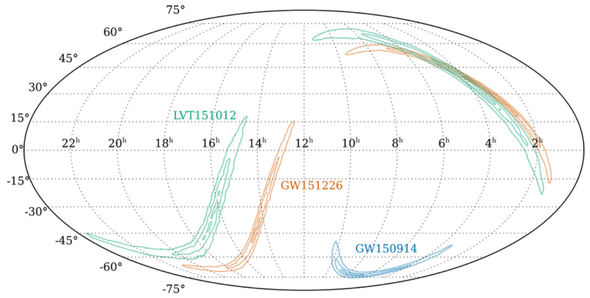

GPS: 1126259462.4

UTC Time: 2015-09-14 09:50

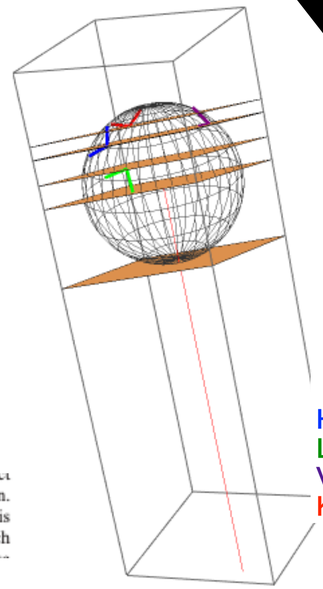

Hanford
Livingston
Virgo
KAGRA

GW150914
delay time (msec) from t0
(+ delay, - advanced)

LHO = 12.8483
LLO = 6.26193

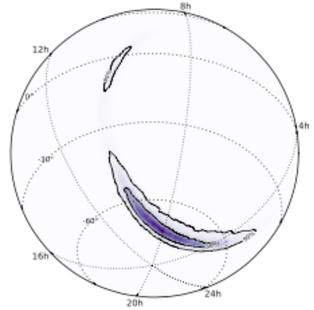

FIG. 4. An orthographic projection of the PDF for the sky location of GW150914 given in terms of right ascension α (measured in hours and labeled around the edge of the figure) and declination δ (measured in degrees and labeled inside the figure). The contours of the 50% and 90% credible regions are plotted over a color-coded PDF. The sky localization forms part of an annulus, set by the time delay of $6.9^{+0.5}_{-0.4}$ ms between the Livingston and Hanford detectors.

PRL 116 (2016) 241102

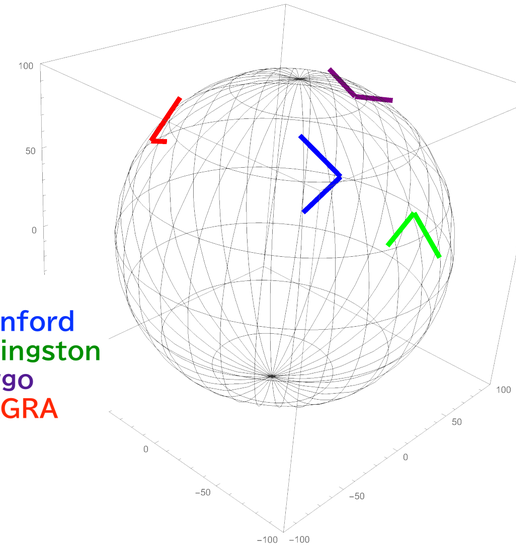

Hanford
Livingston
Virgo
KAGRA

PRL **116,** 221101 (2016) PHYSICAL RE

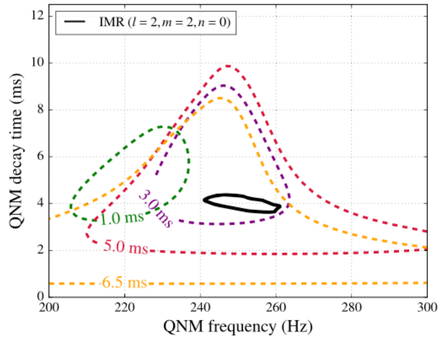

FIG. 5. 90% credible regions in the joint posterior distributions for the damped-sinusoid parameters f_0 and τ (see the main text), assuming start times $t_0 = t_M + 1$, 3, 5, 6.5 ms, where t_M is the merger time of the MAP waveform for GW150914. The black solid line shows the 90% credible region for the frequency and decay time of the $\ell = 2$, $m = 2$, $n = 0$ (i.e., the least-damped) QNM, as derived from the posterior distributions of the remnant mass and spin parameters.

AR法を適用するセグメント長と結果の違い

GW250114_082203

Hanford

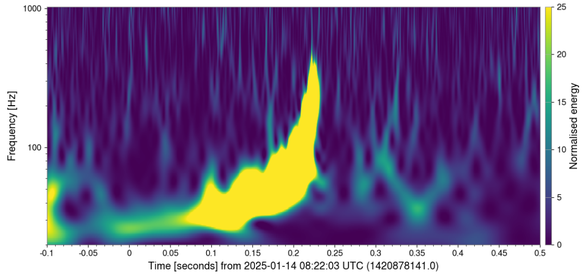

1. セグメント時刻を中央値で表示しているので，実合体時刻＋セグメント長/2 が合体時刻と示される
2. セグメントが長いと，短命なリングダウン波は，周波数候補の首位に表れにくくなる
3. セグメントが短いと，突発的なノイズを多く拾うようになる

1 segment = 512 points
= 1/8 sec = 125 ms

H3

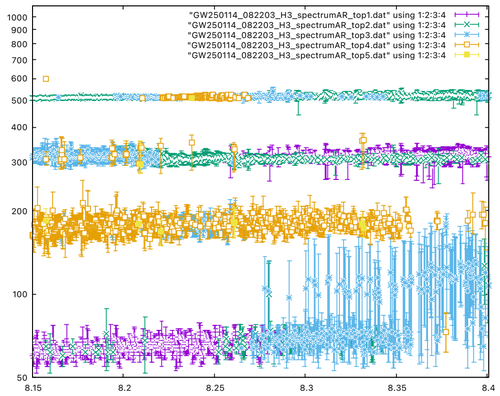

1 segment = 256 points
= 1/16 sec = 62.5 ms

H4

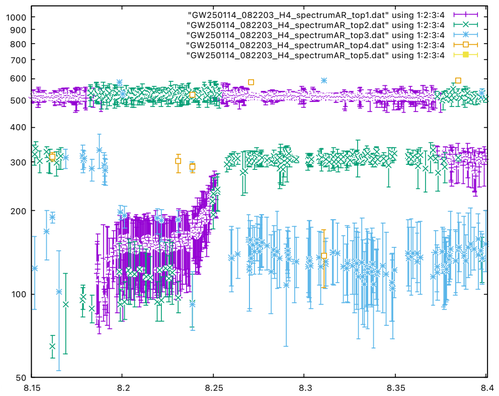

1 segment = 128 points
= 1/32 sec = 31.25 ms

H5

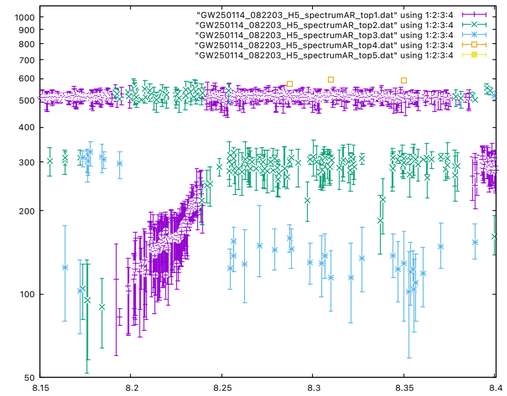

1 segment = 64 points
= 1/64 sec = 15.625 ms

H6

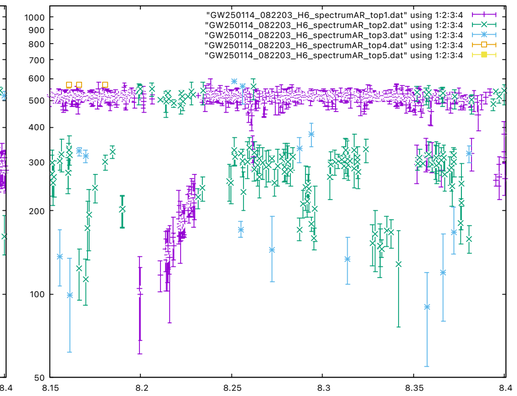

1 segment = 32 points
= 1/128 sec = 7.8125 ms

H7

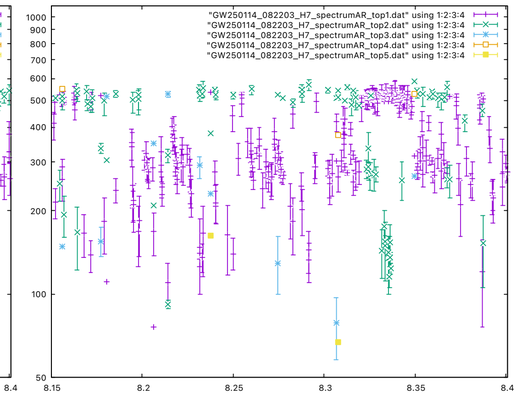

AR法を適用するセグメント長と結果の違い

GW250114_082203

Livingston

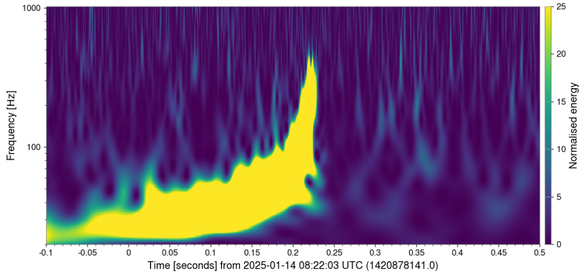

1. セグメント時刻を中央値で表示しているので，実合体時刻＋セグメント長/2 が合体時刻と示される
2. セグメントが長いと，短命なリングダウン波は，周波数候補の首位に表れにくくなる
3. セグメントが短いと，突発的なノイズを多く拾うようになる

1 segment = 512 points
= 1/8 sec = 125 ms

L3

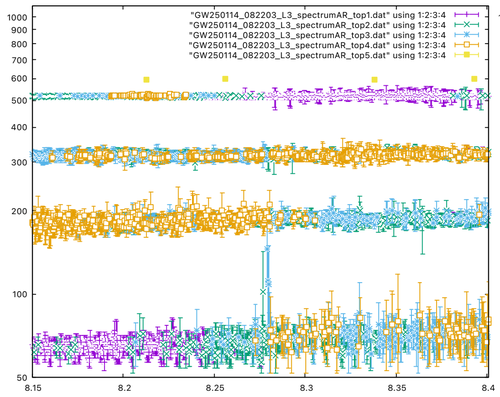

1 segment = 256 points
= 1/16 sec = 62.5 ms

L4

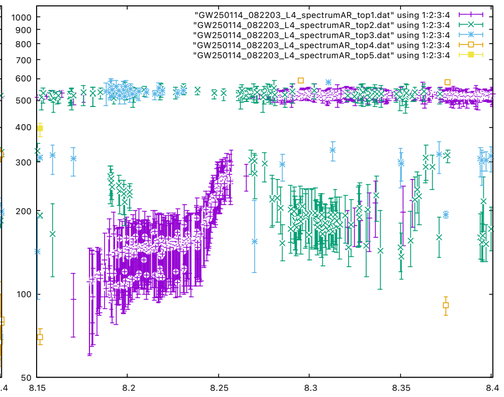

1 segment = 128 points
= 1/32 sec = 31.25 ms

L5

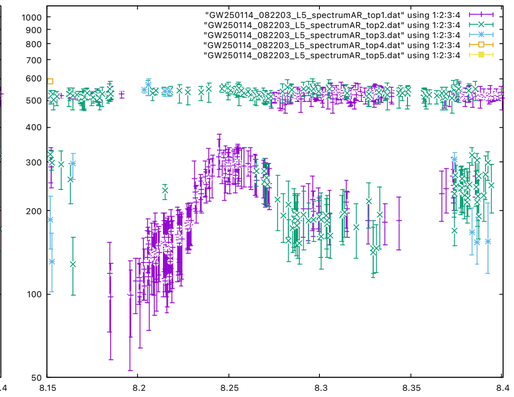

1 segment = 64 points
= 1/64 sec = 15.625 ms

L6

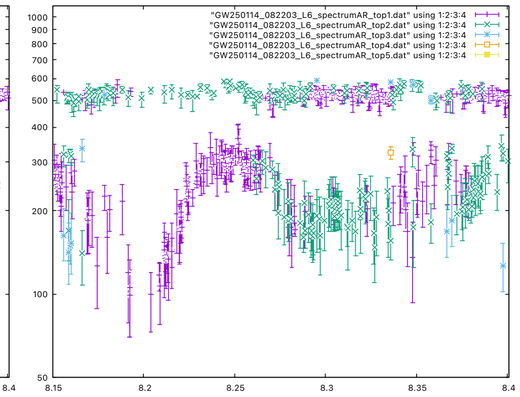

1 segment = 32 points
= 1/128 sec = 7.8125 ms

L7

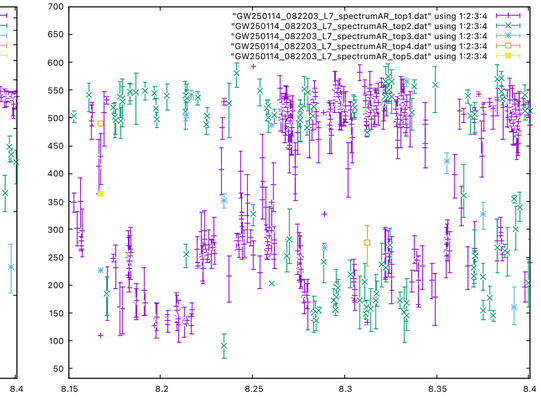

GW230814_230901

SNR=43.0

LV paper ▶ $(M, a, z) = (58.6^{+1.8}_{-1.7}, 0.68^{+0.02}_{-0.03}, 0.06^{+0.02}_{-0.02})$

Livingston only

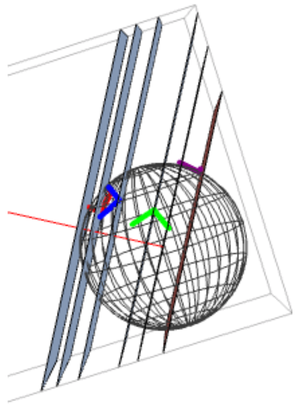

GW230814_230901
delay time (msec) from t0
(+ delay, - advanced)

LHO = -13.0429
LLO = -4.1575
Virgo= 5.58498
KAGRA= -17.847

data file t_merger if 8.8 s
LHO mergertime = 8.78696
LLO mergertime = 8.79584

LLO mergertime = 8.8075 ->
t_merger = 8.8116 s

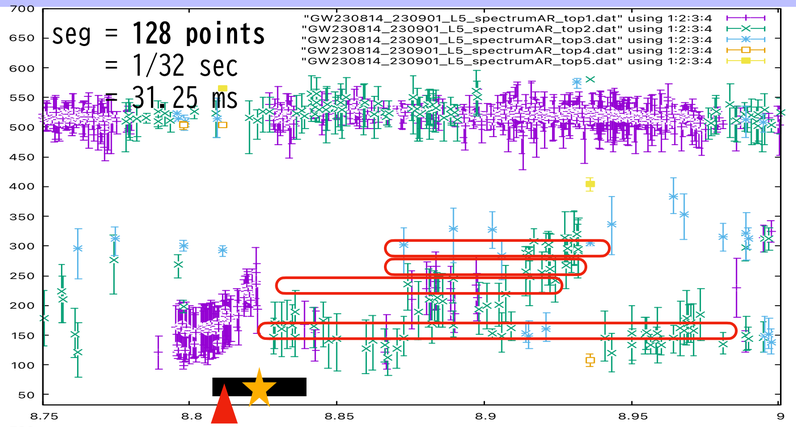

13 segments
f = 309.90 +- 13.62 Hz
t = 8.882 -- 8.941

33 segments
f = 267.33 +- 10.79 Hz
t = 8.883 -- 8.938

44 segments
f = 253.99 +- 11.92 Hz
t = 8.874 -- 8.938

19 segments
f = 163.38 +- 8.43 Hz
t = 8.831 -- 8.971

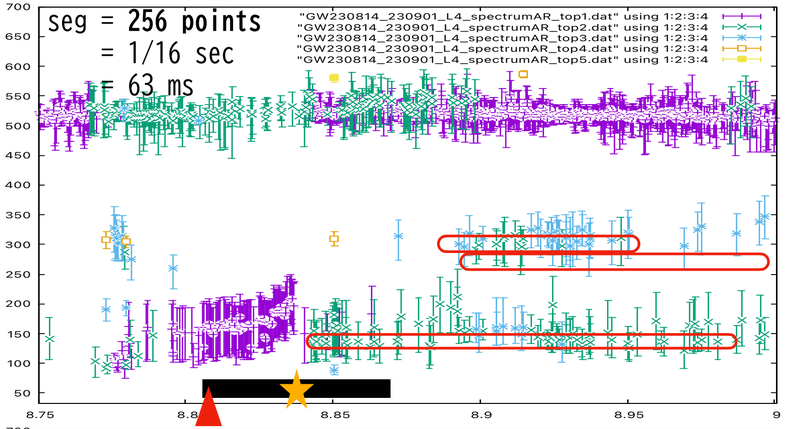

26 segments
f = 318.65 +- 5.79 Hz
t = 8.872 -- 8.951

32 segments
f = 262.05 +- 9.49 Hz
t = 8.898 -- 8.944

28 segments
f = 156.70 +- 7.67 Hz
t = 8.841 -- 8.978

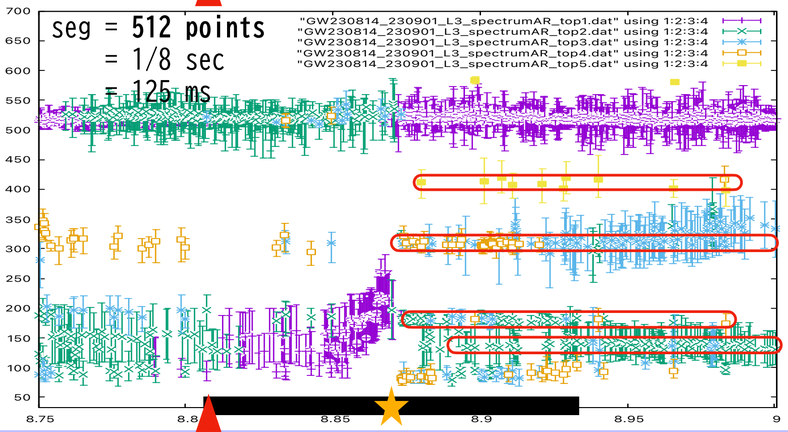

13 segments
f = 412.26 +- 5.12 Hz
t = 8.880 -- 8.984

64 segments
f = 323.89 +- 6.84 Hz
t = 8.874 -- 9.006

9 segments
f = 189.44 +- 6.42 Hz
t = 8.871 -- 8.978

26 segments
f = 133.43 +- 1.56 Hz
t = 8.895 -- 9.014

f_{QNM} @Earth ▶

QNM frequencies [Hz] and decay time [ms] in the detector frame

	frequency [Hz]		
(ℓ, m)	$n=0$	$n=1$	$n=2$
$(2,2)$	274.	267.9	256.2
$(2,1)$	236.5	228.2	213.4
$(2,0)$	204.6	193.4	174.1
$(2,-1)$	180.6	165.7	140.9
$(2,-2)$	161.7	142.	110.2
$(3,3)$	434.6	430.9	424.3
$(3,2)$	392.1	387.8	379.4
$(3,1)$	355.7	350.	339.3
$(3,0)$	325.1	317.8	304.1
$(4,4)$	590.	587.1	581.7
$(4,3)$	543.3	540.2	534.2
$(4,2)$	503.3	499.6	492.6
$(4,1)$	468.	463.4	454.4
$(4,0)$	437.4	431.8	421.2

	decay time [ms]		
(ℓ, m)	$n=0$	$n=1$	$n=2$
$(2,2)$	20.82	6.856	4.051
$(2,1)$	20.73	6.81	3.94
$(2,0)$	20.33	6.636	3.852
$(2,-1)$	19.72	6.551	3.663
$(2,-2)$	19.24	6.163	3.42
$(3,3)$	20.29	6.602	3.664
$(3,2)$	20.14	6.661	3.938
$(3,1)$	20.06	6.623	3.936
$(3,0)$	19.4	6.41	3.798
$(4,4)$	19.91	6.626	3.956
$(4,3)$	19.83	6.584	3.921
$(4,2)$	19.86	6.597	3.938
$(4,1)$	19.55	6.488	3.862
$(4,0)$	19.13	6.349	3.777

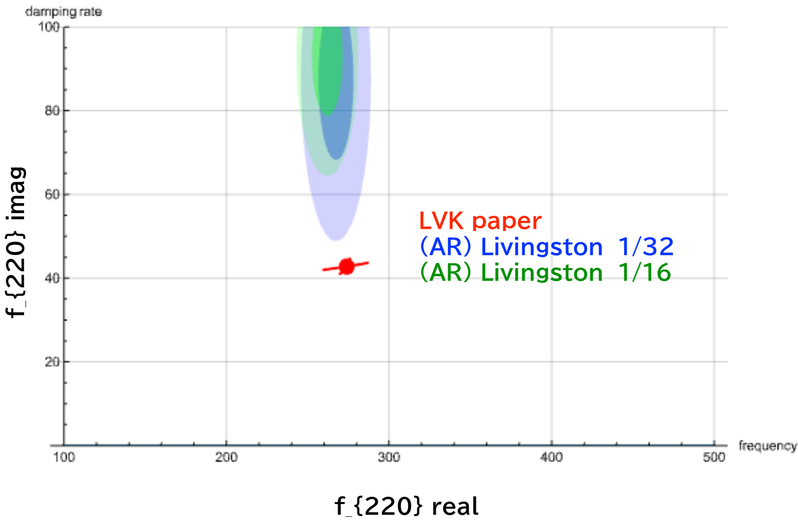

GW230914_111401

SNR=17.7

LV paper ▶ $(M, a, z) = (91.2^{+13.9}_{-9.7}, 0.71^{+0.12}_{-0.12}, 0.45^{+0.22}_{-0.19}$

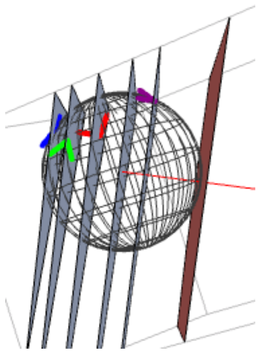

Hanford

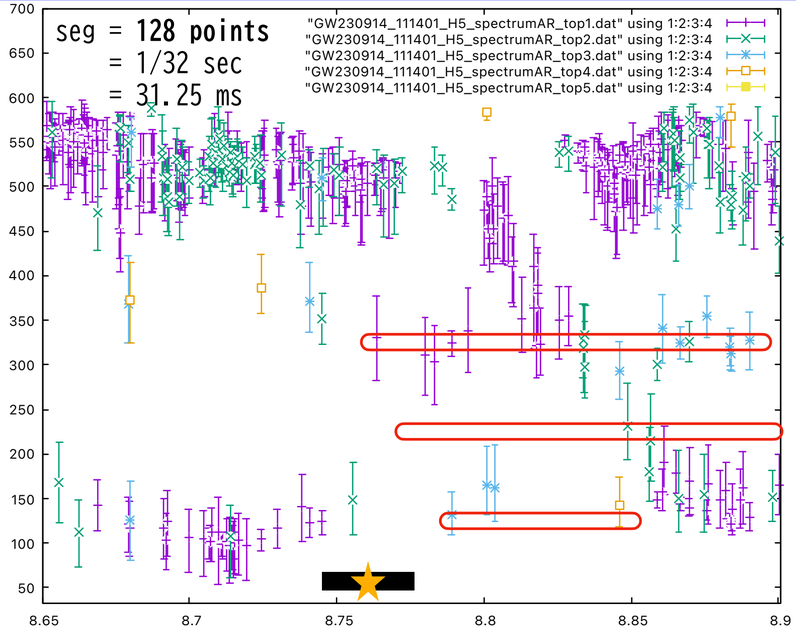

Livingston

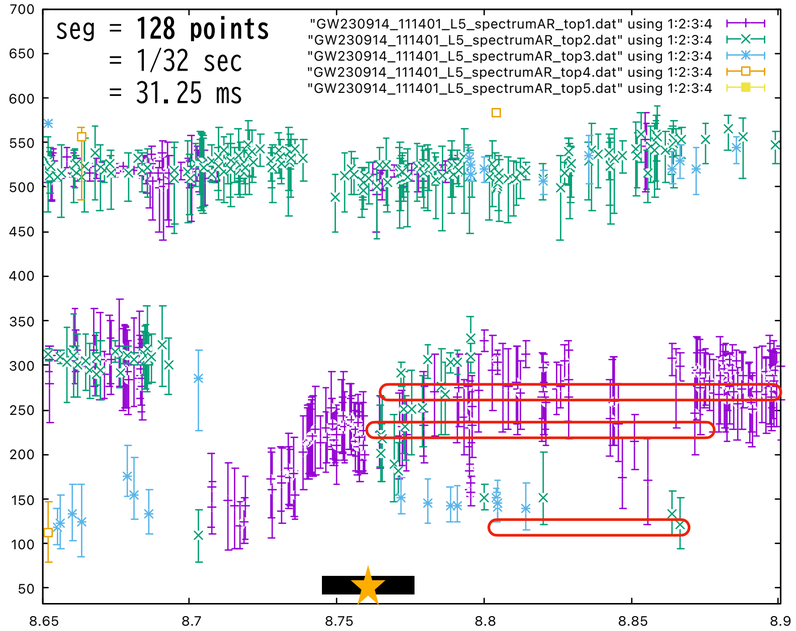

GW230914_111401
delay time (msec) from t0
(+ delay, - advanced)

LHO = 18.6607
LLO = 14.5
Virgo= - 6.2312
KAGRA= 7.98064

data file t_merger if 8.7 s
LHO mergertime = 8.71866
LLO mergertime = 8.7145

f_{QNM} @Earth ▶

27 segments
f = 323.32 +- 14.87 Hz
t = 8.763 -- 8.910

12 segments
f = 220.89 +- 11.79 Hz
t = 8.761 -- 8.908

2 segments
f = 135.54 +- 4.51 Hz
t = 8.789 -- 8.846

35 segments
f = 276.44 +- 9.15 Hz
t = 8.778 -- 8.907

9 segments
f = 222.14 +- 7.54 Hz
t = 8.763 -- 8.869

2 segments
f = 135.24 +- 4.06 Hz
t = 8.814 -- 8.864

QNM frequencies [Hz] and decay time [ms] in the detector frame

	frequency [Hz]		
(ℓ, m)	$n=0$	$n=1$	$n=2$
$(2,2)$	131.8	129.2	124.
$(2,1)$	112.5	108.8	102.1
$(2,0)$	96.49	91.32	82.36
$(2,-1)$	84.69	77.74	66.13
$(2,-2)$	75.45	66.09	51.02
$(3,3)$	208.7	207.1	204.3
$(3,2)$	187.	185.1	181.3
$(3,1)$	168.5	165.9	160.9
$(3,0)$	153.2	149.8	143.4
$(4,4)$	283.3	282.1	279.7
$(4,3)$	259.5	258.1	255.5
$(4,2)$	239.2	237.5	234.2
$(4,1)$	221.4	219.3	215.1
$(4,0)$	206.1	203.5	198.5

	decay time [ms]		
(ℓ, m)	$n=0$	$n=1$	$n=2$
$(2,2)$	24.05	7.927	4.696
$(2,1)$	23.87	7.853	4.55
$(2,0)$	23.27	7.597	4.414
$(2,-1)$	22.47	7.464	4.172
$(2,-2)$	21.91	7.01	3.885
$(3,3)$	23.47	7.627	4.261
$(3,2)$	23.24	7.691	4.55
$(3,1)$	23.04	7.612	4.528
$(3,0)$	22.18	7.332	4.346
$(4,4)$	23.03	7.671	4.583
$(4,3)$	22.9	7.608	4.532
$(4,2)$	22.87	7.603	4.542
$(4,1)$	22.43	7.444	4.433
$(4,0)$	21.87	7.261	4.321

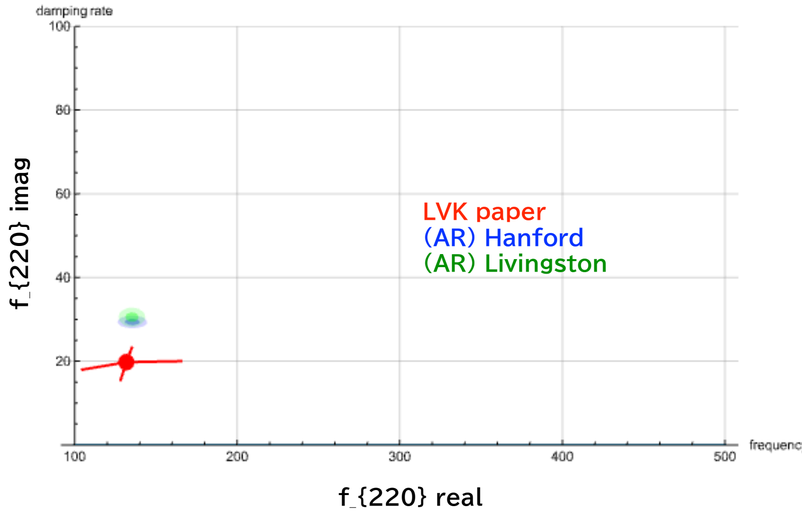

GW230927_153832

SNR=21.5

LV paper ▶ $(M, a, z) = (36.6^{+3.2}_{-2.2}, 0.69^{+0.04}_{-0.03}, 0.23^{+0.06}_{-0.1})$

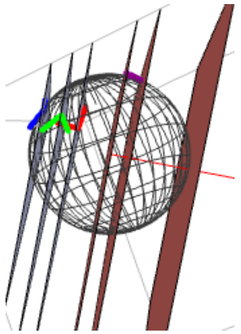

Hanford

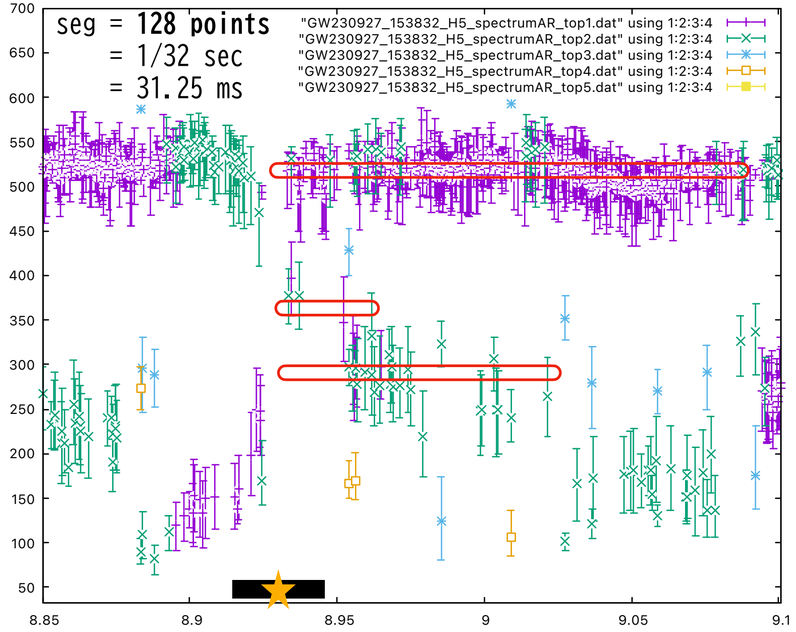

Livingston

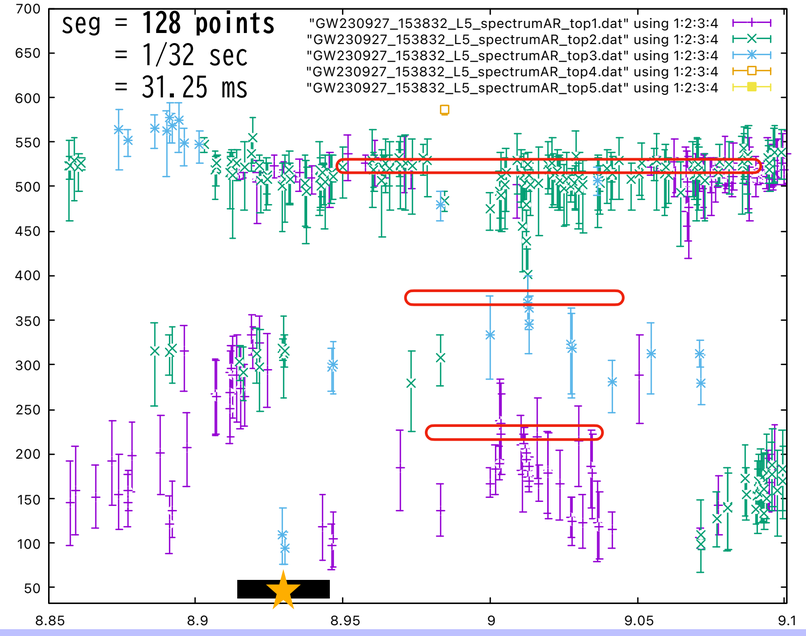

GW230927_153832
delay time (msec) from t0
(+ delay, - advanced)

LHO = 18.9786
LLO = 14.1019
Virgo = -4.88992
KAGRA = 9.72756

data file t_merger if 8.9 s
LHO mergertime = 8.91898
LLO mergertime = 8.9141

f_{QNM} @Earth ▶

63 segments
f = 528.68 +- 5.33 Hz
t = 8.932 -- 9.073

7 segments
f = 359.15 +- 15.36 Hz
t = 8.930 -- 8.952

26 segments
f = 280.35 +- 12.52 Hz
t = 8.929 -- 9.021

21 segments
f = 528.83 +- 4.52 Hz
t = 8.942 -- 9.071

5 segments
f = 379.10 +- 10.57 Hz
t = 8.926 -- 9.049

11 segments
f = 232.79 +- 9.50 Hz
t = 8.977 -- 9.014

QNM frequencies [Hz] and decay time [ms] in the detector frame

	frequency [Hz]		
(ℓ, m)	$n=0$	$n=1$	$n=2$
$(2,2)$	381.	372.8	357.
$(2,1)$	327.7	316.4	296.3
$(2,0)$	282.7	267.3	240.8
$(2,-1)$	249.	228.6	194.4
$(2,-2)$	222.6	195.3	151.3
$(3,3)$	604.	599.1	590.2
$(3,2)$	543.7	537.9	526.5
$(3,1)$	492.1	484.4	469.7
$(3,0)$	449.	439.	420.2
$(4,4)$	820.	816.2	808.8
$(4,3)$	753.8	749.6	741.5
$(4,2)$	697.1	692.1	682.4
$(4,1)$	647.3	641.	628.6
$(4,0)$	604.2	596.5	581.8

	decay time [ms]		
(ℓ, m)	$n=0$	$n=1$	$n=2$
$(2,2)$	11.26	3.709	2.193
$(2,1)$	11.2	3.681	2.131
$(2,0)$	10.97	3.579	2.078
$(2,-1)$	10.62	3.528	1.972
$(2,-2)$	10.36	3.317	1.84
$(3,3)$	10.98	3.571	1.986
$(3,2)$	10.89	3.602	2.13
$(3,1)$	10.83	3.577	2.126
$(3,0)$	10.46	3.456	2.048
$(4,4)$	10.77	3.586	2.141
$(4,3)$	10.72	3.561	2.121
$(4,2)$	10.73	3.565	2.129
$(4,1)$	10.55	3.502	2.085
$(4,0)$	10.31	3.423	2.037

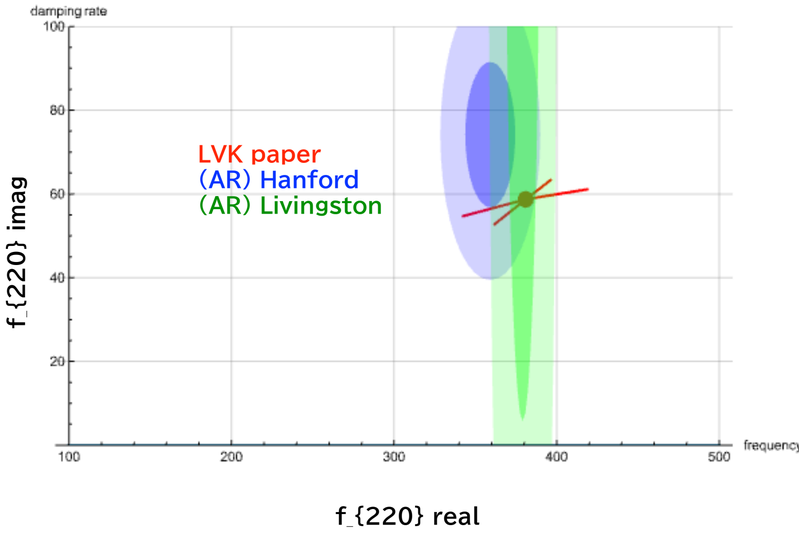

GW231028_153006

SNR=22.9

LV paper ▶

$(M, a, z) = (146.^{+23.}_{-14.}, 0.84^{+0.05}_{-0.1}, 0.61^{+0.24}_{-0.23})$

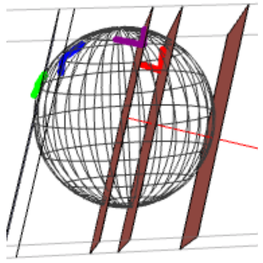

Hanford

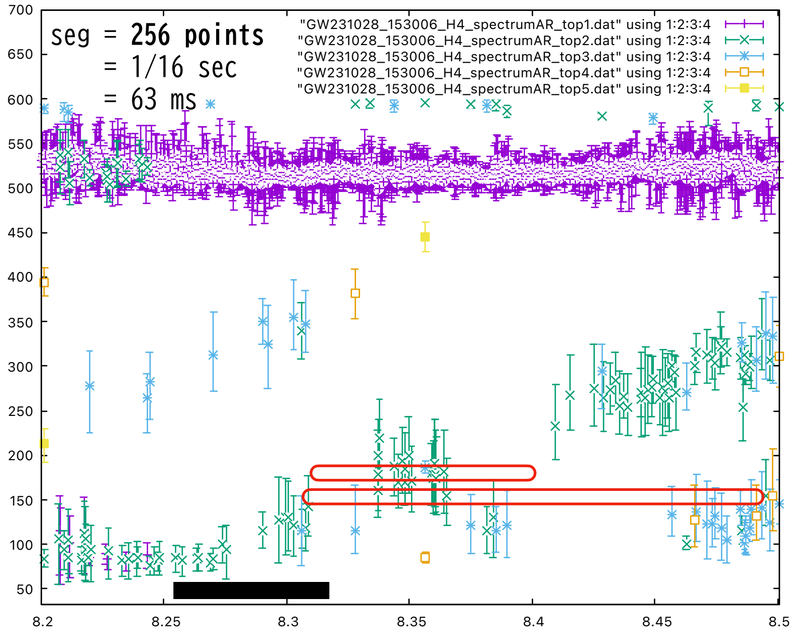

f_{QNM} @Earth ▶

13 segments
f = 180.46 +- 11.50 Hz
t = 8.315 -- 8.401

5 segments
f = 144.36 +- 4.28 Hz
t = 8.309 -- 8.499

QNM frequencies [Hz] and decay time [ms] in the detector frame

	frequency [Hz]		
(ℓ, m)	$n=0$	$n=1$	$n=2$
$(2,2)$	84.16	83.3	81.5
$(2,1)$	67.52	65.72	62.63
$(2,0)$	55.5	52.78	47.9
$(2,-1)$	47.41	43.57	37.09
$(2,-2)$	41.32	35.85	27.08
$(3,3)$	132.1	131.6	130.7
$(3,2)$	113.8	113.	111.4
$(3,1)$	99.11	97.71	94.95
$(3,0)$	87.74	85.9	82.4
$(4,4)$	179.	178.6	177.9
$(4,3)$	159.3	158.7	157.7
$(4,2)$	142.7	141.8	140.1
$(4,1)$	129.1	127.9	125.6
$(4,0)$	117.9	116.4	113.7

	decay time [ms]		
(ℓ, m)	$n=0$	$n=1$	$n=2$
$(2,2)$	38.88	12.91	7.739
$(2,1)$	37.44	12.43	7.315
$(2,0)$	34.66	11.36	6.629
$(2,-1)$	32.55	10.8	6.033
$(2,-2)$	31.71	10.1	5.565
$(3,3)$	38.3	12.34	7.148
$(3,2)$	37.13	12.34	7.349
$(3,1)$	35.25	11.68	6.977
$(3,0)$	32.97	10.91	6.474
$(4,4)$	37.69	12.58	7.539
$(4,3)$	36.95	12.3	7.354
$(4,2)$	35.78	11.92	7.159
$(4,1)$	33.95	11.28	6.734
$(4,0)$	32.45	10.78	6.418

Livingston

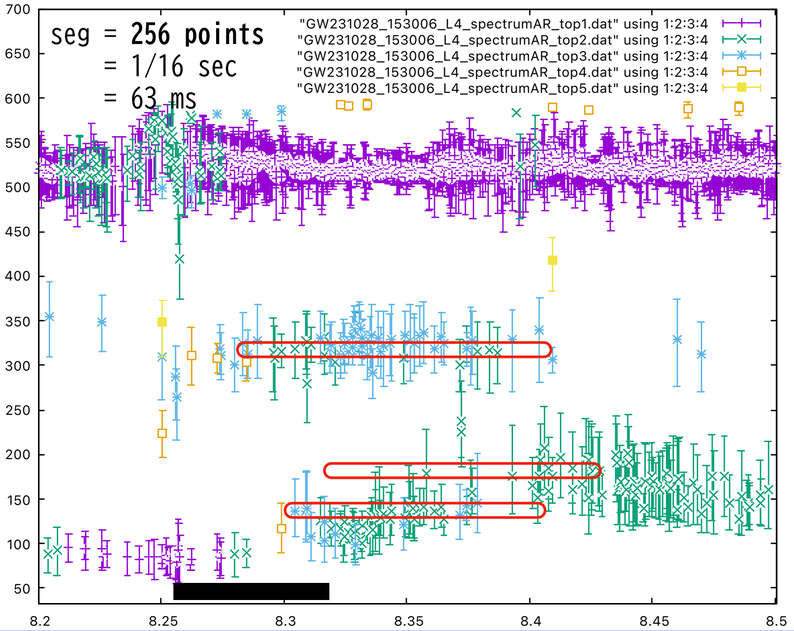

53 segments
f = 324.62 +- 11.78 Hz
t = 8.276 -- 8.408

27 segments
f = 189.77 +- 14.37 Hz
t = 8.335 -- 8.425

12 segments
f = 135.84 +- 3.96 Hz
t = 8.305 -- 8.395

GW231028_153006
delay time (msec) from t0
(+ delay, - advanced)

LHO = 17.1862
LLO = 20.494
Virgo= 0.0273621
KAGRA= -6.52488

data file t_merger if 8.2 s
LHO mergertime = 8.21719
LLO mergertime = 8.22049

Too massive, and low-frequency

GW231206_233901

SNR=22.9

LV paper ▶ $(M, a, z) = (63.6^{+5.1}_{-3.4}, 0.67^{+0.06}_{-0.07}, 0.28^{+0.05}_{-0.08})$

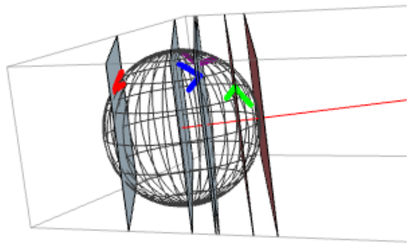

Hanford

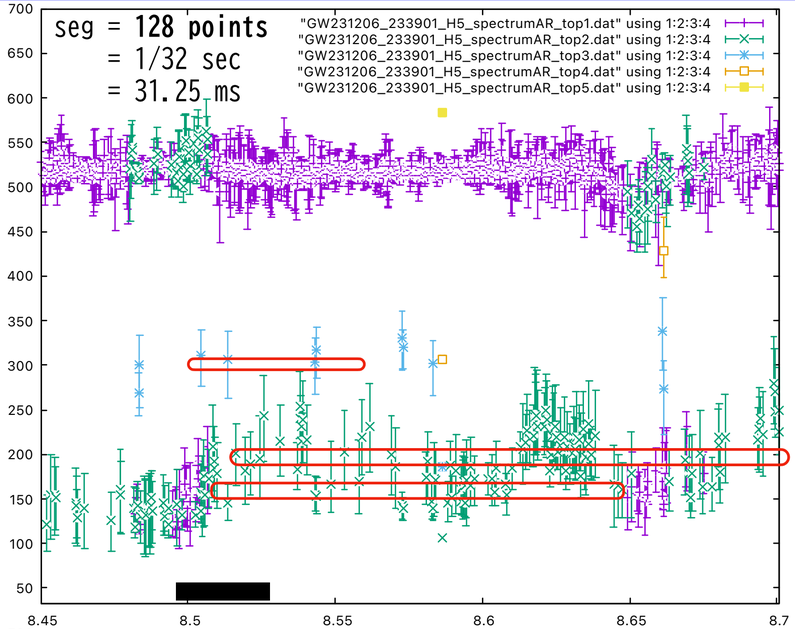

16 segments
f = 297.82 +- 23.26 Hz
t = 8.516 -- 8.561

98 segments
f = 214.24 +- 11.92 Hz
t = 8.515 -- 8.695

26 segments
f = 165.33 +- 14.37 Hz
t = 8.504 -- 8.649

Livingston

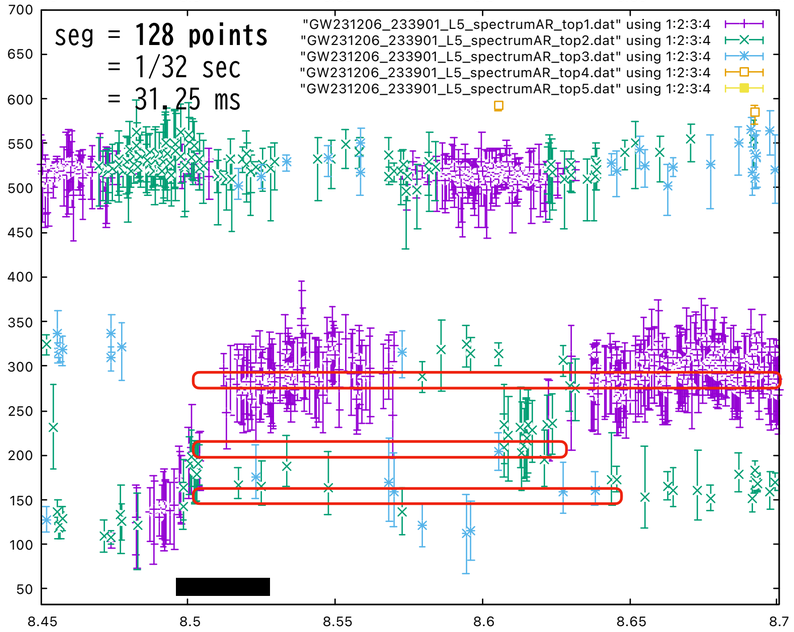

128 segments
f = 292.48 +- 11.97 Hz
t = 8.511 -- 8.648

44 segments
f = 216.65 +- 13.17 Hz
t = 8.500 -- 8.626

17 segments
f = 172.18 +- 21.42 Hz
t = 8.501 -- 8.644

GW231206_233901
delay time (msec) from t0
(+ delay, - advanced)

LHO = -6.80343
LLO = -15.3679
Virgo= -6.07737
KAGRA= 16.6444

data file t_merger if 8.2 s
LHO t_merger = 8.1932
LLO t_merger = 8.18463

f_{QNM} @Earth ▶

QNM frequencies [Hz] and decay time [ms] in the detector frame.

	frequency [Hz]		
(ℓ, m)	$n=0$	$n=1$	$n=2$
(2, 2)	207.5	202.7	193.6
(2, 1)	179.7	173.3	161.9
(2, 0)	155.9	147.3	132.6
(2, −1)	137.9	126.5	107.6
(2, −2)	123.7	108.7	84.47
(3, 3)	329.2	326.4	321.2
(3, 2)	297.7	294.4	287.9
(3, 1)	270.6	266.3	258.
(3, 0)	247.8	242.2	231.7
(4, 4)	447.	444.7	440.5
(4, 3)	412.3	409.9	405.3
(4, 2)	382.6	379.8	374.4
(4, 1)	356.3	352.8	345.9
(4, 0)	333.4	329.1	321.

	decay time [ms]		
(ℓ, m)	$n=0$	$n=1$	$n=2$
(2, 2)	18.63	6.133	3.621
(2, 1)	18.56	6.095	3.525
(2, 0)	18.24	5.952	3.454
(2, −1)	17.71	5.885	3.291
(2, −2)	17.29	5.54	3.076
(3, 3)	18.15	5.907	3.271
(3, 2)	18.02	5.96	3.523
(3, 1)	17.97	5.934	3.526
(3, 0)	17.41	5.752	3.407
(4, 4)	17.8	5.925	3.537
(4, 3)	17.74	5.89	3.507
(4, 2)	17.78	5.906	3.524
(4, 1)	17.53	5.816	3.461
(4, 0)	17.17	5.697	3.389

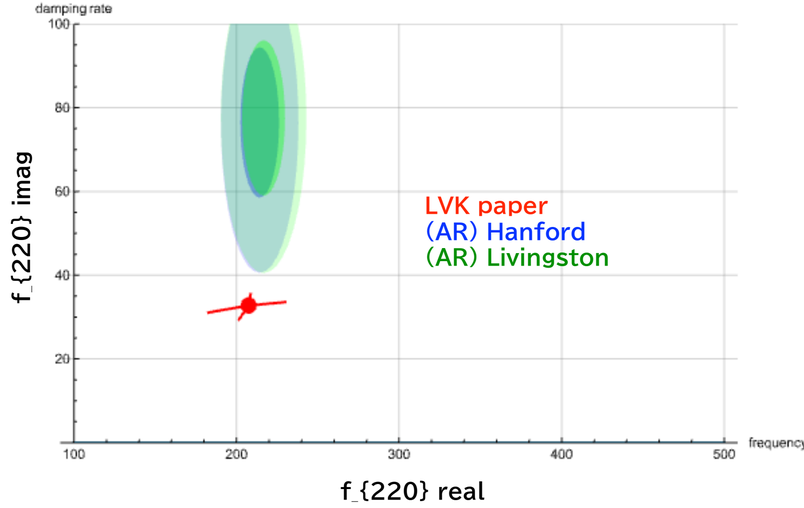

GW231226_101520

SNR=34.7

LV paper ▶

$(M, a, z) = (71.^{+3.1}_{-2.3}, 0.67^{+0.04}_{-0.04}, 0.22^{+0.03}_{-0.05})$

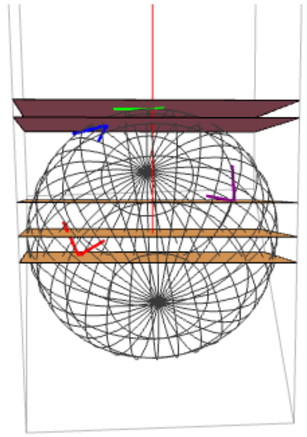

Hanford

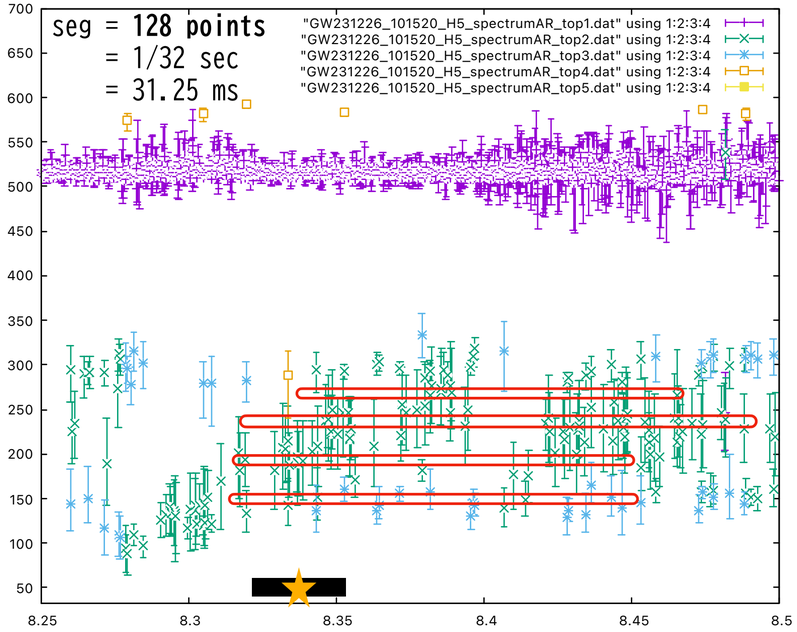

f_{QNM} @Earth ▶

15 segments
f = 278.45 +- 5.14 Hz
t = 8.349 -- 8.470

116 segments
f = 240.89 +- 9.80 Hz
t = 8.329 -- 8.474

10 segments
f = 196.00 +- 12.64 Hz
t = 8.329 -- 8.456

11 segments
f = 151.14 +- 10.18 Hz
t = 8.325 -- 8.453

Livingston

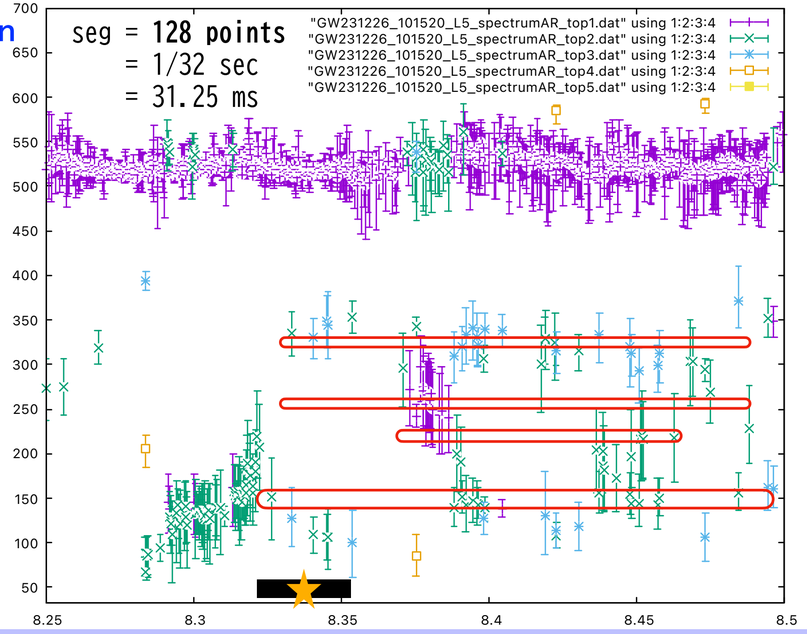

14 segments
f = 318.15 +- 11.86 Hz
t = 8.330 -- 8.474

69 segments
f = 245.97 +- 11.61 Hz
t = 8.334 -- 8.470

34 segments
f = 216.13 +- 10.19 Hz
t = 8.386 -- 8.465

16 segments
f = 154.42 +- 18.69 Hz
t = 8.326 -- 8.458

GW231226_101520
delay time (msec) from t0
(+ delay, - advanced)

LHO = -18.6083
LLO = -21.2684
Virgo= -5.42538
KAGRA= 4.15996

data file t_merger if 8.3 s
LHO t_merger = 8.28139
LLO t_merger = 8.27873

QNM frequencies [Hz] and decay time [ms] in the detector frame

	frequency [Hz]		
(ℓ, m)	$n=0$	$n=1$	$n=2$
$(2,2)$	195.	190.5	181.9
$(2,1)$	168.9	162.9	152.2
$(2,0)$	146.5	138.4	124.6
$(2,-1)$	129.6	118.9	101.1
$(2,-2)$	116.2	102.1	79.39
$(3,3)$	309.4	306.7	301.8
$(3,2)$	279.8	276.7	270.6
$(3,1)$	254.3	250.2	242.5
$(3,0)$	232.9	227.6	217.8
$(4,4)$	420.1	418.	414.
$(4,3)$	387.5	385.2	380.9
$(4,2)$	359.6	356.9	351.8
$(4,1)$	334.9	331.6	325.1
$(4,0)$	313.4	309.3	301.7

	decay time [ms]		
(ℓ, m)	$n=0$	$n=1$	$n=2$
$(2,2)$	21.82	7.183	4.241
$(2,1)$	21.74	7.139	4.129
$(2,0)$	21.37	6.972	4.045
$(2,-1)$	20.75	6.893	3.854
$(2,-2)$	20.25	6.489	3.603
$(3,3)$	21.25	6.919	3.831
$(3,2)$	21.11	6.981	4.126
$(3,1)$	21.05	6.95	4.129
$(3,0)$	20.39	6.737	3.99
$(4,4)$	20.85	6.939	4.142
$(4,3)$	20.78	6.899	4.108
$(4,2)$	20.82	6.917	4.128
$(4,1)$	20.53	6.812	4.054
$(4,0)$	20.1	6.673	3.97

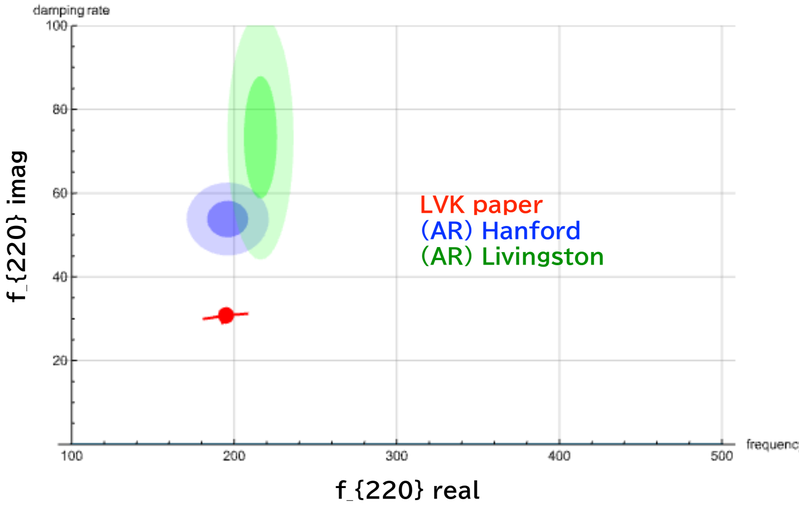

GW250114_082203

SNR=78.5

1 segment = 128 points
= 1/32 sec = 31.25 ms

LV paper ▶ $(M, a, z) = (62.7^{+1}_{-1.1}, 0.68^{+0.01}_{-0.01}, 0.09^{+0.01}_{-0.01})$

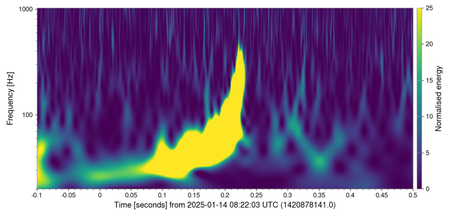

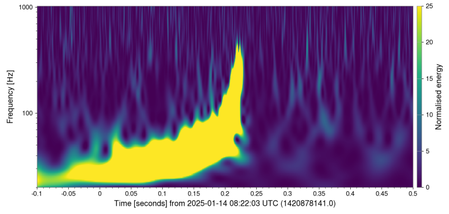

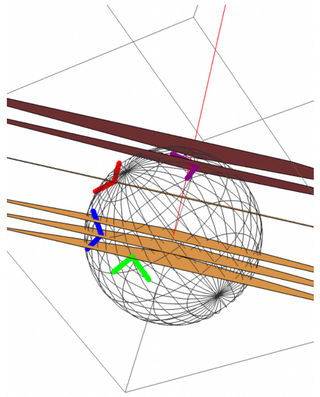

GW250114_082203
delay time (msec) from t0
(+ delay, - advanced)

LHO = 3.10759
LLO = 6.12127
Virgo= -17.2618
KAGRA= -9.36207

data file t_merger if 8.20 s
LHO t_merger = 8.20311
LLO t_merger = 8.20612

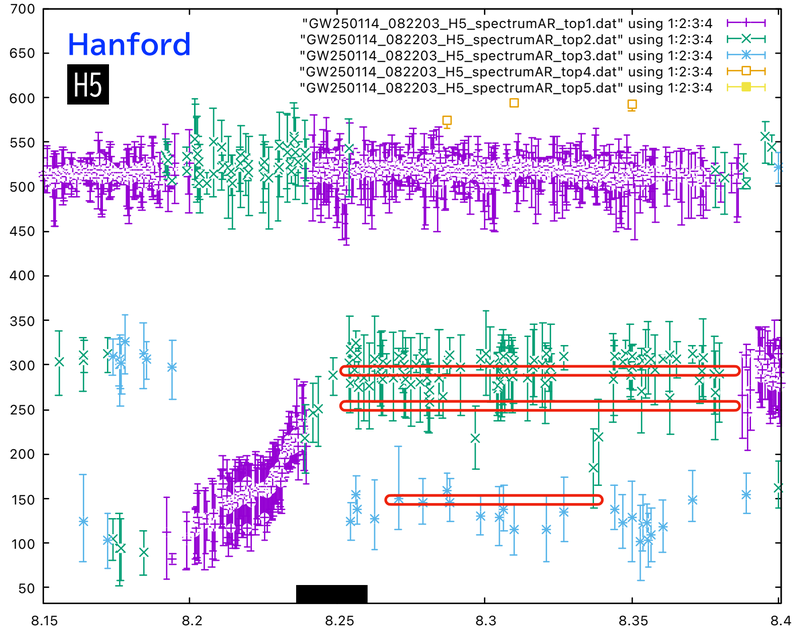

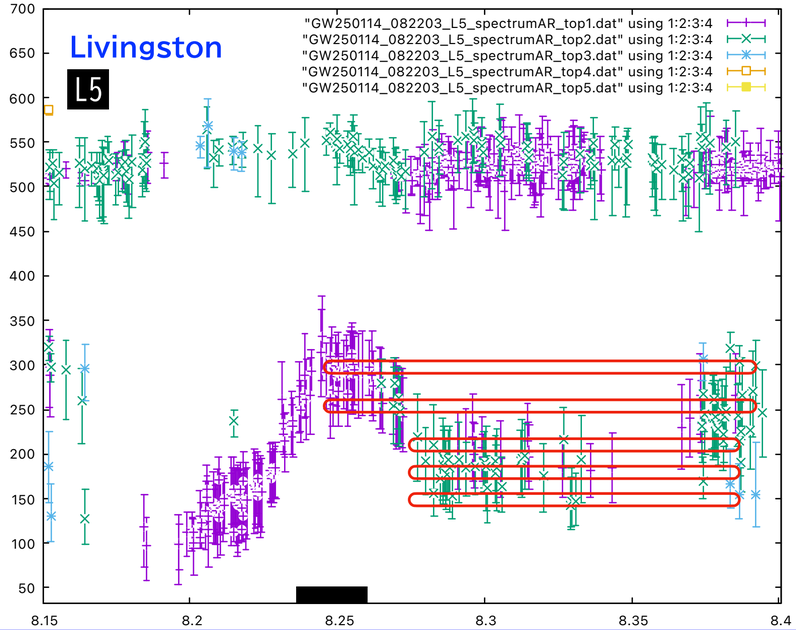

90 segments
f = 296.79 +- 7.21 Hz
t = 8.248 -- 8.380

31 segments
f = 252.94 +- 9.38 Hz
t = 8.249 -- 8.388

5 segments
f = 141.37 +- 4.30 Hz
t = 8.271 -- 8.344

44 segments
f = 294.25 +- 9.48 Hz
t = 8.246 -- 8.392

95 segments
f = 251.02 +- 12.76 Hz
t = 8.248 -- 8.395

59 segments
f = 212.00 +- 8.43 Hz
t = 8.271 -- 8.387

22 segments
f = 176.53 +- 19.44 Hz
t = 8.275 -- 8.386

8 segments
f = 147.73 +- 7.92 Hz
t = 8.265 -- 8.386

f_{QNM} @Earth ▶

QNM frequencies [Hz] and decay time [ms] in the detector frame

	frequency [Hz]		
(ℓ, m)	$n=0$	$n=1$	$n=2$
$(2,2)$	249.	243.5	232.9
$(2,1)$	215.	207.4	194.
$(2,0)$	185.9	175.8	158.3
$(2,-1)$	164.1	150.6	128.1
$(2,-2)$	147.	129.	100.1
$(3,3)$	395.	391.6	385.6
$(3,2)$	356.4	352.5	344.8
$(3,1)$	323.3	318.1	308.4
$(3,0)$	295.4	288.8	276.4
$(4,4)$	536.2	533.6	528.7
$(4,3)$	493.8	491.	485.6
$(4,2)$	457.5	454.1	447.7
$(4,1)$	425.4	421.2	413.
$(4,0)$	397.6	392.5	382.8

	decay time [ms]		
(ℓ, m)	$n=0$	$n=1$	$n=2$
$(2,2)$	21.67	7.134	4.215
$(2,1)$	21.57	7.085	4.099
$(2,0)$	21.16	6.904	4.008
$(2,-1)$	20.52	6.817	3.811
$(2,-2)$	20.02	6.413	3.559
$(3,3)$	21.11	6.87	3.812
$(3,2)$	20.96	6.931	4.097
$(3,1)$	20.87	6.891	4.096
$(3,0)$	20.18	6.67	3.952
$(4,4)$	20.71	6.895	4.116
$(4,3)$	20.63	6.851	4.079
$(4,2)$	20.66	6.864	4.097
$(4,1)$	20.35	6.751	4.018
$(4,0)$	19.9	6.606	3.931

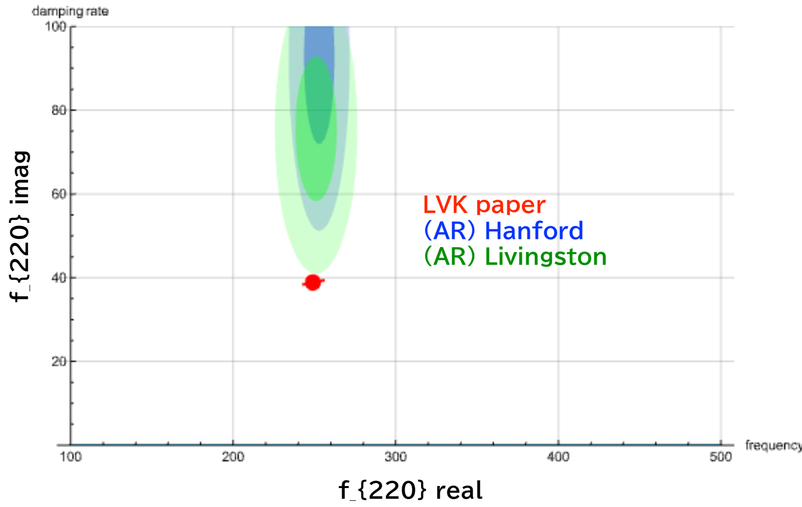

(2,2,1) は (2,2,0)と判別できない
(4,4,0) はノイズ帯のようで，見えたとは言い難い
(3,0,0) はHanford/Livingston双方で見えている

higher-order modes

$$h_+(\iota,\varphi_0;t) - ih_x(\iota,\varphi_0;t) = \sum_{\ell=2}^{\infty}\sum_{m=-\ell}^{\ell} {}_{-2}Y_{\ell m}(\iota,\varphi_0)h_{\ell m}(t)$$

PHYSICAL REVIEW D **98,** 084028 (2018)

Enriching the symphony of gravitational waves from binary black holes by tuning higher harmonics

Roberto Cotesta,[1,*] Alessandra Buonanno,[1,2] Alejandro Bohé,[1] Andrea Taracchini,[1] Ian Hinder,[1] and Serguei Ossokine[1]
[1]*Max Planck Institute for Gravitational Physics (Albert Einstein Institute), Am Mühlenberg 1, Potsdam 14476, Germany*
[2]*Department of Physics, University of Maryland, College Park, Maryland 20742, USA*

(Received 9 April 2018; published 17 October 2018)

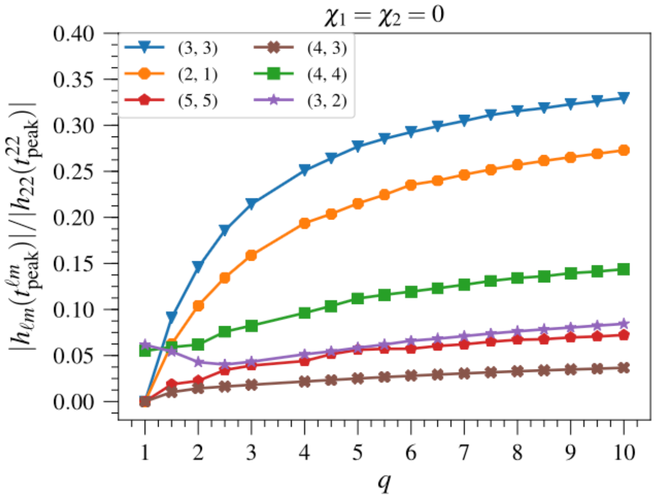

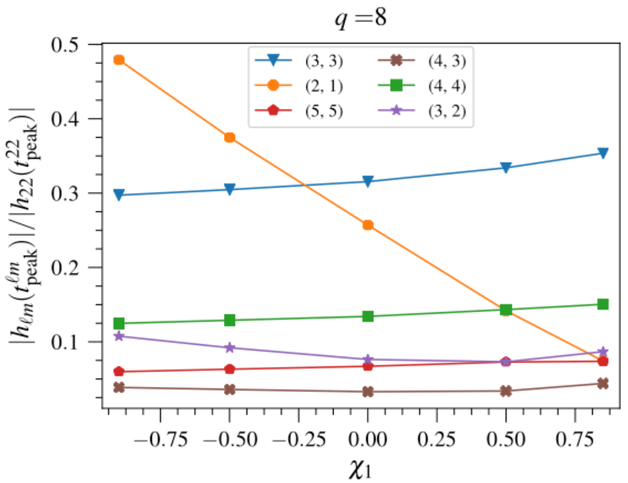

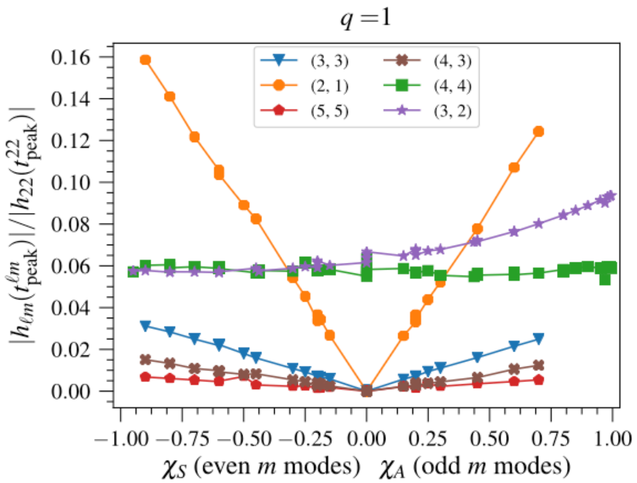

等質量，スピンなし連星の場合，m=奇数　は発生しない

well-known mode hierarchy (2,2),(3,3),(2,1),(4,4),(3,2),(5,5),(4,3)ではない

$r = {}_{-2}Y^2_2(\theta,\phi)$　$r = {}_{-2}Y^1_2(\theta,\phi)$　$r = {}_{-2}Y^0_2(\theta,\phi)$　$r = {}_{-2}Y^3_3(\theta,\phi)$　$r = {}_{-2}Y^2_3(\theta,\phi)$　$r = {}_{-2}Y^1_3(\theta,\phi)$　$r = {}_{-2}Y^0_3(\theta,\phi)$　$r = {}_{-2}Y^4_4(\theta,\phi)$

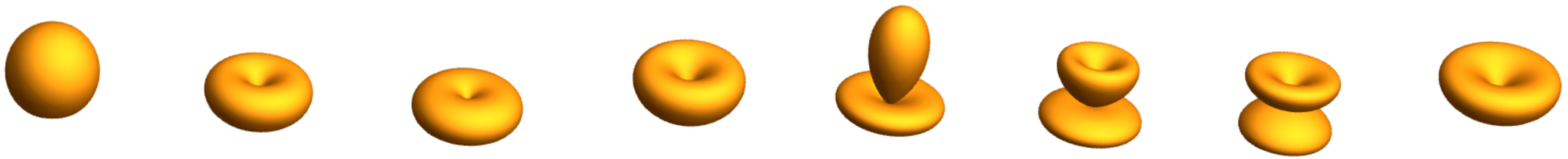

まとめと展望

自己回帰モデル（AR法）

$$x_n = a_1 x_{n-1} + a_2 x_{n-2} + \cdots + a_M x_{n-M} + \varepsilon = \sum_{j=1}^{M} a_j x_{n-j} + \varepsilon$$

ノイズを含む短時間実データ 64 pts (16ms), 128pts (32ms) に対しても, 周波数と減衰率を抽出できる
データのみを用いていて, テンプレートは不要(理論に独立). 複数のモードも抽出可能.
検出器ごとのデータ解析. 波形抽出の時刻も明確にできる.

LVK O4a: リングダウン波形の抽出を試みた.

S/N >= 15 (インスパイラル部含む)のイベントに対しては, リングダウン波形は取り出せる.
(時間幅 [merger time + 200 ms], Band Filterings [20-600Hz] など
parameterはイベントごとに設定せず共通)

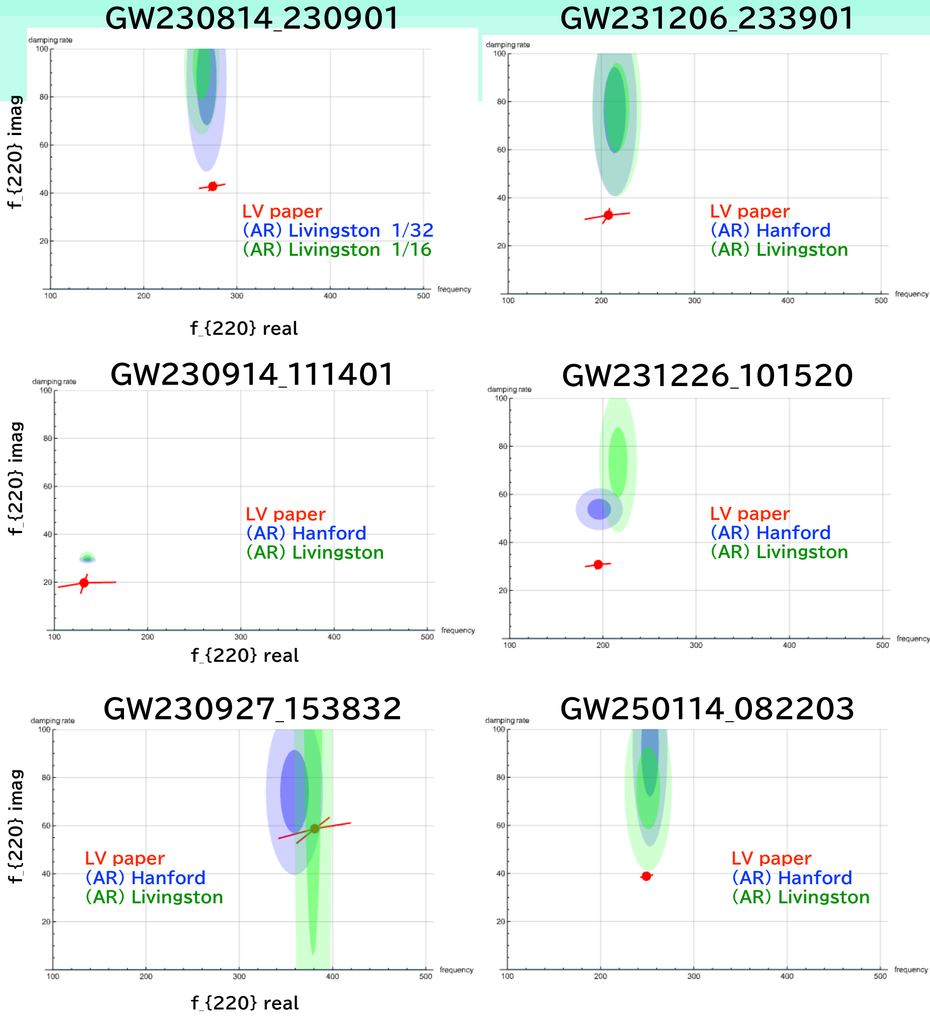

AR法はリングダウン波を抽出しているか Yes
2干渉計(Hanford, Livingston) で合致した値になるか Yes
LVK catalogと合致した値になるか Almost Yes

➡ **f_imag (減衰率)は大きく見積もる傾向がある.**

リングダウン波の開始時刻はいつか 3ms-5ms
高次モード, 高調波モードはみつかるか 見えているものもある
GRと矛盾しないか 今のところ consistent といえる

GW250114_082203について
(2,2,1) は (2,2,0)と判別できない
(4,4,0) はノイズ帯のようで, 見えたとは言い難い
(3,0,0) はHanford/Livingston双方で見えている

➡ **他の方法との整合性check**

➡ **どのモードが励起されたのか, しくみを含めて考える研究へ**